New therapeutic and diagnostic approaches with which to influence mitochondrial dysfunctions

Eszter Tuboly

Ph.D. Thesis

University of Szeged, Faculty of Medicine
Doctoral School of Multidisciplinary Medicine

Supervisor:
Prof. Dr. Mihály Boros

University of Szeged, Institute of Surgical Research
Szeged

2014

LIST OF FULL PAPERS RELATED TO THE SUBJECT OF THE THESIS

I. Tuboly E, Mészáros A, Boros M. Nonbacterial biotic methanogenesis, possible mechanisms and significance. In: Methanogenesis. Biochemistry, Ecological Functions, Natural and Engineered Environments. Badalians G.G. (ed.). Nova Science Publishers, Inc. NY, USA 2014, Chapter 2, pp. 19-49. ISBN 978-1-63321-567-2. **IF: 0**

II. Tőkés T, **Tuboly E,** Varga G, Major L, Ghyczy M, Kaszaki J, Boros M. Protective effects of L-alpha-glycerylphosphorylcholine on ischaemia-reperfusion-induced inflammatory reactions. Eur J Nutr. 2014 (E-pub ahead of print) **IF: 3.127**

III. Tőkés T, Varga G, Garab D, Nagy Z, Fekete G, **Tuboly E**, Plangár I, Mán I, Szabó RE, Szabó ZI, Volford G, Ghyczy M, Kaszaki J, Boros M, Hideghéty K: Peripheral inflammatory activation after hippocampus irradiation in the rat. Int J Radiat Biol. 2014; 90(1):1-6.

IF: 1.895

IV. Tuboly E, Szabó A, Erős G, Mohácsi A, Szabó G, Tengölics R, Rákhely G, Boros M. Determination of endogenous methane formation by photoacoustic spectroscopy. J Breath Res. 2013; 7(4):046004. **IF: 3.590**

V. Tuboly E, Szabó A, Garab D, Bartha G, Janovszky Á, Erős G, Szabó A, Mohácsi Á, Szabó G, Kaszaki J, Ghyczy M, Boros M. Methane biogenesis during sodium azide-induced chemical hypoxia in rats. Am J Physiol Cell Physiol. 2013; 304(2):C207-214. **IF: 3.715**

VI. Boros M, **Tuboly E**, Mészáros A, Amann A: The role of methane in mammalian physiology - is it a gasotransmitter? *J Breath Res.* **(under review)**

LIST OF ABSTRACTS RELATED TO THE SUBJECT OF THE THESIS

I. Tuboly E, Babik B, Bartha G, Kisvari G, Serédi V, Mohácsi Á, Szabó A, Végh Á, Szabó G, Boros M: Methane release in humans under oxido-reductive stress conditions. *J Surg Res.* 2014; 2:592-593.

II. Tuboly E, Kozlov A, Dungel P, Singer K, Váradi D, Erdély E, Boros M: The effects of L-α-glycerylphosphorylcholine in stress states accompanied by mitochondrial dysfunction. *Shock.* 2013; 40 (1):40.

III. Tuboly E, Babik B, Bartha G, Kisvari G, Serédi V, Mohácsi Á, Szabó A, Végh Á, Szabó G, Boros M: Átmeneti hypoxiát követő metánképződés szívműtéten átesett betegekben. *Magy. Seb.* 2013; p.114.

IV. **Tuboly E**, Babik B, Bartha G, Kisvari G, Serédi V, Mohácsi Á, Szabó A, Végh Á, Szabó G, Boros M: Methane release in humans under oxido-reductive stress conditions. *Eur. Surg. Res.* 2013. 2013; 50 (suppl 1) 1-162 (2013) p.8.

V. Tőkés T, Varga G, Garab D, **Tuboly E**, Plangár I, Mán I, Szabó Z, Kaszaki J, Ghyczy M, Hideghéthy K, Boros M: L-alfa glicerilfoszforilkolin protektív hatása hippocampus irradiáción átesett patkány modellben. *Magy. Seb.* 2013; 66 (2013) 2 p.111.

VI. Tőkés T, Varga G, Fekete G, Nagy Z, **Tuboly E**, Szigeti E, Ghyczy M, Kaszaki J, Boros M, Hideghéty K: Protective effects of L-α-glycerylphosphorylcholine after hippocampus irradiation *Shock*. 2011; 36:33.

VII. Varga G, Tőkés T, **Tuboly E**, Major L, Ghyczy M, Kaszaki J, Boros M: Protective effects of α-glycerylphosphorylcholine in mesenteric ischaemia-reperfusion. *Shock.* 2011; 36:34.

VIII. Tőkés T, Varga G, **Tuboly E**, Major L, Ghyczy M, Kaszaki J, Boros M: Anti-inflammatory effects of l-alpha glycerylphosphorylcholine in mesenteric ischemia/reperfusion *Acta Phys. Scand.* 2011; 202:121.

IX. Tőkés T, Varga G, **Tuboly E**, Ghyczy M, Kaszaki J, Boros M: Az L-α-glicerilfoszforilkolin mikrokeringésre gyakorolt protektív hatása mesenteialis ischaemia során. *Magy. Seb.* 2011; 64:152.

X. Tőkés T, Varga G, **Tuboly E**, Major L, Ghyczy M, Kaszaki J, Boros M: Protective effect of L-α-glycerylphosphorylcholine against ischaemia-reperfusion injury in the rat small intestine *Fiziologia-Physiology* (suppl.). 2011; 1223-2076.

XI. Major L, Tőkés T, Varga G, **Tuboly E**, Ghyczy M, Kaszaki J, Boros M: Az L-α-glicerilfoszforilkolin preventív mikrokeringésre gyakorolt hatása a mesenterialis ischaemia során. *Érbetegségek.* (suppl.) 2011; 1:17.

OTHER PAPERS RELATED TO THE FIELD OF THE THESIS

I. Varga G, Érces D, **Tuboly E**, Kaszaki J, Ghyczy M, Boros M. Characterization of the antiinflammatory properties of methane inhalation during ischaemia-reperfusion. Magy Seb. 2012; 65(4):205-11. **IF: 0**

II. Szabó A, Ruzsanyi V, Unterkofler K, Mohácsi Á, **Tuboly E,** Boros M, Szabó G, Hinterhuber H, Amann A**:** Exhaled methane concentration profiles during exercise on an ergometer. *J Breath Res.* **(under review)**

CONTENTS

LIST OF ABBREVIATIONS

ATP: adenosine triphosphate

bw: body weight

CH_4: methane

CO_2: carbon dioxide

CO: carbon monoxide

CT: computer tomography

DTT: dithiotreitol

EDTA: ethylenediaminetetraacetic acid

EMG: electrophilic methyl group

FCD: functional capillary density

GC: gas chromatography

GI: gastrointestinal

GPC: glycerylphosphorylcholine

H_2: hydrogen

H_2O_2: hydrogen peroxide

H_2S: hydrogen disulfide

H_2SO_4: sulfuric acid

HCl: hydrogen chloride

He-Ne: helium-neon

ip: intraperitoneally

iv: intravenously

IR: ischemia/reperfusion

IVM: intravital videomicroscopy

K_2CO_3: potassium carbonate

K_3PO_4: potassium phosphate

LPS: lipopolysaccharide

METC: mitochondrial electron transport chain

$MgSO_4$: magnesium sulfate

MPO: myeloperoxidase

mtDNA: mitochondrial DNA

NAD: nicotinamide adenine dinucleotide

$NaN_{3:}$ sodium azide

NBT: nitroblue tetrazolium

NO: nitric oxide

$O_2^{\cdot -}$: superoxide anion

PAS: photoacoustic spectroscopy

PC: phosphatidylcholine

PMN: polymorphonuclear

PMSF: phenylmethylsulfonyl fluoride

ppm: part per million

PTP: permeability transition pore

RBCV: red blood cell velocity

RNS: reactive nitrogen species

ROS: reactive oxygen species

sc: subcutaneously

SMA: superior mesenteric artery

XOR: xanthine oxidoreductase

SUMMARY

Methane (CH_4) was earlier thought to be produced in the gastrointestinal (GI) tract by methanogenic bacterial fermentation, under strictly anaerobic conditions. Humans can be CH_4 producers or CH_4 nonproducers, depending on the presence of methanogenic strains, age, race and lifestyle. The producer status, or a higher CH_4 level in the exhaled breath, is considered to be associated with various GI disorders, such as chronic constipation or lactose malabsorption. Nevertheless, the exclusivity of bacterial CH_4 formation was challenged recently when *in vitro* and *in vivo* studies revealed the possibility of non-microbial CH_4 formation in mitochondria and eukaryote cells, in both plants and animals.

The classical CH_4 detection method is based on gas chromatography, which has many limitations, and real-time measurement is not possible. We set out to develop a photoacoustic spectroscopy (PAS)-based on-line method with appropriate specificity and sensitivity to describe the process of CH_4 emission in rodents and also in human volunteers.

Our next objective was to investigate nonbacterial biotic methanogenesis and to shed light on the mechanistic details of the reaction. The initial *in vitro* studies led to the proposal that a continuous lack of the electron acceptor oxygen will maintain an elevated mitochondrial $NADH/NAD^+$ ratio, causing reductive stress. Electrophilic methyl groups bound to positively-charged nitrogen moieties, such as in phosphatidylcholine molecules, may potentially act as substitute electron acceptors, and in consequence CH_4 may be liberated. Thus, priming during hypoxia occurs as a progressive process involving depressed electron transport, the loss of cytochrome c and antioxidants, and the triggering of methane release during the abnormal formation of reactive oxygen species induced by reoxygenation or reperfusion. We therefore hypothesized that the formation and emission of CH_4 in mammals may be connected with hypoxic events leading to, or associated with a mitochondrial dysfunction.

A further aim was to influence the consequences of mitochondrial dysfunction by the administration of a water-soluble, deacylated derivative of phosphatidylcholine, L-alpha-glycerylphosphorylcholine (GPC). Here, we took into account the earlier *in vivo* findings that GPC is a centrally-acting cholinergic precursor which increases the tolerance to ischemic tissue damage and is clinically effective in various neurodegenerative diseases. We assumed that GPC treatment could moderate the CH_4 generation and also the inflammatory consequences of experimental oxidoreductive stress.

In three parallel studies, we determined data on the applicability of a novel PAS-based instrument. As compared with gas chromatography, this allows real-time and dynamic measurements, while the gas-sampling procedure does not demand the use of disposable bags or syringes and operates without chemicals. The use of the instrument is noninvasive, allows the detection of the whole-body gas emission of rodents and is appropriate for human exhaled breath analysis too. Moreover, it is relatively cost-effective due to the application of near-infrared diode lasers.

After the development of an appropriately specific and sensitive detection system for CH_4, we investigated the functional role of mitochondrial electron transport in biogenesis. We demonstrated that the extent of CH_4 generation is significantly increased in rodents exposed to chronic sodium azide challenge or endotoxemia. The phenomenon proved to be independent of the methanogenic flora, since the CH_4 emission was also elevated in antibiotic-treated groups. As endotoxemia and specific inhibition of mitochondrial complex IV with sodium azide led to an increased CH_4 output, we assumed that mitochondrial distress and the subsequent inflammatory reaction might be common denominators of CH_4 biogenesis. The results pointed to a possible role of CH_4 as an alarm signal for the development of mitochondrial responses under hypoxic conditions, and accordingly it may be a biomarker of such events.

In our studies, the stress-induced CH_4 generation, the hepatic microcirculatory reduction and the increased pro-oxidant and inflammatory responses were markedly attenuated by GPC treatment. When the consequence of mesenteric ischemia/reperfusion, or gamma-irradiation of the hippocampus were investigated, it emerged that GPC maintained the decreased ATP content of the liver.

In conclusion, the results suggest that PAS-based spectroscopy is an excellent approach for CH_4 detection, not only in animal experiments, but also in human investigations. CH_4 production in mammals is connected with hypoxic events and is associated with a mitochondrial dysfunction. GPC is protective against the inflammatory consequences of a hypoxic reaction that might involve cellular or mitochondrial CH_4 generation.

I. INTRODUCTION

1.1.1. Mitochondria, characteristics and functions

Mitochondria are membrane-enclosed organelles, the energy-producing centers in almost all eukaryotic cells. The outer membrane fully surrounds the inner membrane, with a small intermembrane space between, and the inner membrane is loaded with protein complexes of the mitochondrial electron transport chain (METC) and adenosine triphosphate (ATP) synthesis. This membrane surrounds the matrix, where the citric acid cycle produces the electrons that travel from one protein complex to the next. The outer membrane has many protein-based pores that allow the passage of ions and molecules as large as a small protein. In contrast, the permeability of the inner membrane is restricted, much like the plasma membrane of a cell.

According to the endosymbiontic theory, the evolutionary emergence of mitochondria is a result of the endocytosis of alpha-proteobacteria. Phylogenetic investigations support this assumption, but on the other hand, there are several characteristic features which refer to prokaryotic ancestors. Indeed, the barrel-shaped mitochondrion with a diameter of 0.5 to 1.0 μm is bacterium-like. It has its own independent set of double-stranded mitochondrial DNA (mtDNA), which is uniquely not linear, but circular in form. The number of DNA copies in one mitochondrion can vary from 2 to 10, depending on the energy-requirements of the given cell type. It is also a common feature with prokaryotic organisms that there are no introns in the genetic material, and the ratio of the encoding region is therefore much higher. Nevertheless, the genome size of mtDNA is significantly smaller than the nuclear, especially in humans, where it contains 16, 569 nucleotides. The number of encoding genes is only 37, which encode no more than 13 proteins, all belonging in the METC. However, this system needs more proteins for optimal action, which will arrive from the cell nucleus. These include the enzymes required for the citric acid cycle, the proteins involved in DNA replication and transcription, and ribosomal proteins. The protein complexes of the METC are a mixture of proteins encoded by mitochondrial genes and proteins encoded by nuclear genes. Proteins in both the outer and inner mitochondrial membranes facilitate the transport of newly synthesized, unfolded proteins from the cytoplasm into the matrix, where folding ensues. Accordingly, mitochondria are under strong gene expression and operating regulation of the nuclear genome. A further point of interest is that the genetic inheritance of mitochondria in mammals is exclusively maternal, because at the time of fertilization, the paternal mtDNA disappears by a still unknown mechanism. Additionally, there is no exonuclease activity in the

mitochondria, and the mutation rate is therefore approximately 10-fold higher than in the nuclear genome. This might be the main reason why a series of genetic diseases are mitochondria-dependent.

Nevertheless, several pathological conditions are caused by a mitochondrial dysfunction, independently from mtDNA changes. The METC is of decisive functional importance: it is responsible for all the fundamental physiological processes of the cell, producing chemiosmotic energy through O_2 consumption. In brief, electrons are transported through the complexes of the METC and finally accepted by the O_2, this process leading to ATP synthesis, the exclusive source of cellular energy. In more detail, the electrons pass from complex I, the nicotinamide adenine dinucleotide (NADH) dehydrogenase complex, to a carrier, coenzyme Q, which is embedded in the membrane. From coenzyme Q, the electrons are passed to complex III, the cytochrome bc1 complex, which is associated with another proton translocation event. From complex III, the electrons flow to cytochrome c, and then to complex IV, the cytochrome oxidase complex. More protons are translocated by complex IV, and at this site of the METC, the electron is finally accepted by O_2, along with protons. The O_2 is reduced to H_2O, while the proton gradient is used to generate the proton motive force for ATP synthase. Since O_2 is diatomic, two electron pairs and two cytochrome oxidase complexes are needed to complete the final procedure. This last electron transport step serves the critical function of removing electrons from the system so that electron transport can operate continuously. Complex II, the succinate dehydrogenase complex, is a separate starting point, where the electrons can enter from succinate and flow back to coenzyme Q, and then again to complex III, cytochrome c and complex IV. Thus, there is a common electron transport pathway beyond the two entry points, either complex I or complex II, and a reverse electron flow step between them. In summary, substrate oxidation by the METC creates a proton gradient across the inner membrane, which becomes a driving force for ATP synthesis. For optimal performance, the electron shuttle must be in a steady state as regards the two entry points and the final utilization points, and O_2 availability is therefore crucial.

1.1.2. The Mitochondrial oxidoreductive stress

Oxidative stress is generally defined as an imbalance that favors the production of reactive oxygen species (ROS) over antioxidant defenses; this term is applied to *in vivo* situations in which damage is caused by an elevated level of ROS or other free radical generation, either directly or indirectly. Nevertheless, the majority of ROS are products of mitochondrial respiration. If only one electron is utilized for the reduction of O_2, a relatively

stable intermediate is produced, superoxide anion ($O_2^{\cdot -}$), and approximately 1-2% of the O_2 consumed during normal physiological respiration is converted into this radical (Nohl, 1978).

The METC contains several redox centers that may leak electrons to O_2, serving as the primary source of $O_2^{\cdot -}$ production in most tissues. $O_2^{\cdot -}$ –producing sites and enzymes of the mitochondria have recently been discussed in a comprehensive review (Dröse, 2012). According to the current view, the main source of $O_2^{\cdot -}$ generation is complex I, from where ROS are released into the mitochondrial matrix and the intermembrane space, and the contributions of other complexes and sites seem to be relatively minor. However, others have observed that complex III is significant in ROS formation, and $O_2^{\cdot -}$ production by complex I is markedly stimulated in the presence of succinate, indicating that a reverse electron flow is also involved (Bleier, 2012, Ishii, 2013) (**Figure 1**).

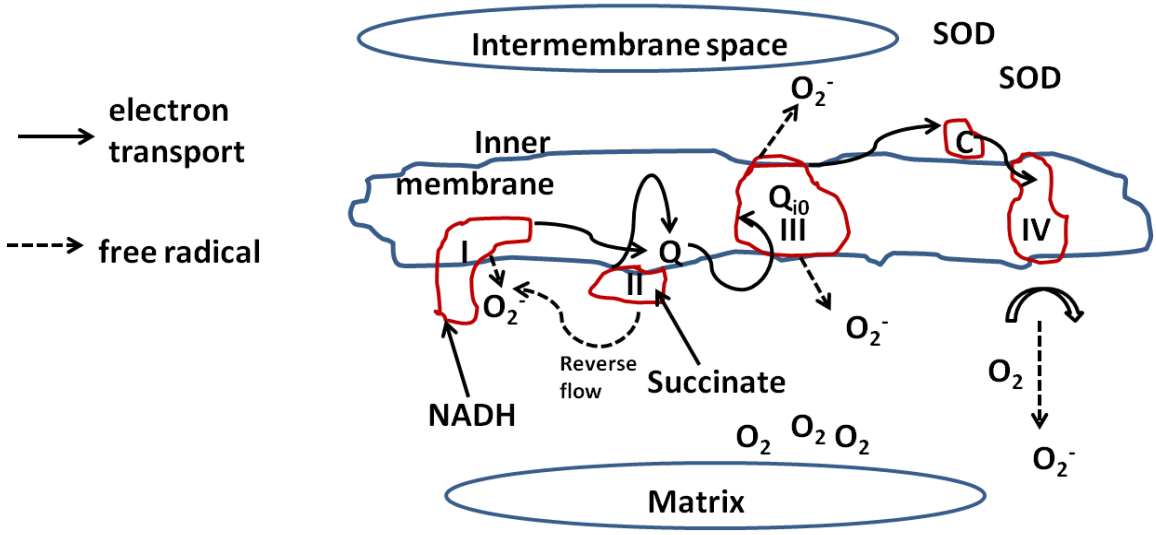

Figure 1. Scheme of the main electron transport steps in the METC and the typical exit points of unpaired valence electrons.

As ROS are produced at significant rates by reactions intrinsic to the normal aerobic metabolism, "redox homeostasis" appropriately includes an intracellular balance between ROS generation and scavenging (Droge, 2006). A major threat to this controlled equilibrium is hypoxia, since the absence of electron acceptor O_2 leads to a shift in reducing potential to a higher than normal reducing power, which may result in a depression of mitochondrial ATP formation and progressive functional and structural cell damage. Re-establishment of O_2 supply, however, is also precarious, as the disturbed intracellular biochemistry may lead to the generation of excess $O_2^{\cdot -}$, which forms the basis of "oxidative stress". The targets of ROS may include proteins, sugars and structure-forming phospholipids, and it is therefore widely accepted that several disease states are linked to oxidative stress, even though the potential of

‘antioxidant’ compounds to prevent or cure ROS-induced processes is very limited (Gutteridge, 1999). Furthermore, ROS are key openers of the mitochondrial permeability transition pores (PTPs), which can result in modification of the permeability properties of the inner membrane and therefore cause pathological mitochondrial states (Halestrap, 2003).

The main consequences of oxidative stress forces are well-established, but the role of lipid peroxidation should be highlighted, especially in the mitochondria, where the highly reactive components of polyunsaturated fatty acids are particularly affected, in both the outer and inner membranes (Bindoli, 1988). This potentially harmful process proceeds by a ROS-mediated chain mechanism, when the multiple double bonds between fatty acids can rapidly be demolished, leading to membrane destruction. In the mitochondria, these vulnerable unsaturated moieties are found mainly in 1-saturated-2-unsaturated-diacylphospholipids and in cardiolipin, which is unsaturated at both positions (Pfeiffer, 1979).

In general terms, mitochondrial dysfunction-associated diseases are mainly due to O_2 deprivation or METC failure, either directly or indirectly, owing to chemicals, toxic gases or circulatory, respiratory system impairments, in a wide range of deleterious processes accompanied by ROS accumulation. Not surprisingly, a mitochondrial dysfunction is implicated in variety of diverse pathologies, including cancers, type II diabetes, cardiovascular diseases, acute or chronic ischemic injuries, and several neurodegenerative diseases (Boland, 2013; Dikalov, 2013; Huang, 2014; Mukherjee, 2013; Ngo, 2013). In addition, ROS play roles in cellular metabolic processes through the inhibition or activation of various enzymatic cascades and several transcriptional factors, which finally makes the condition more severe (Corbi, 2013).

1.1.3. Mitochondrial therapies

Mitochondrion-directed pharmacotherapy is a quite challenging task, because oxidoreductive stress-associated damage may often lead to an irreversible outcome by the time these events are diagnosed. Accordingly, novel therapeutic targets, the development of new and accurate diagnostic approaches, and the identification of new disease markers are equally important to promote appropriate and timely treatment.

The discussion of mtDNA-based genetic disorders is beyond the scope of this thesis, but in non-inherited diseases, several clinically-used drugs can improve or damage the mitochondrial bioenergetics. These drugs can act via regulation of the METC, fatty acid uptake or oxidation, PTPs, ATPase, ion channels and transporters, cardiolipin content, and mtDNA (Wallace, 2008; Toogood, 2008). A number of reviews have discussed these issues in

terms of these molecular targets (Scatena, 2007), off-targets within the cell (Cohen, 2010), or the chemical classification of drugs (Finsterer, 2010). It should be added that several medications in the late clinical phases of drug assessment, and even after acceptance, display unwanted side-effects, and it would be important to understand the role of direct or indirect mitochondrial damage possibly associated with these events. Direct mechanisms include the inhibition of METC complexes, transcriptions of these complexes and enzymes required for glycolysis and β-oxidation. Indirect damage can occur via ROS overproduction or decreases in endogenous antioxidants (Olszewska, 2012). Nevertheless, mitochondrial toxicity tests are still not required for drug approval. Today, the proposed approaches are as follows: 1) the development of preclinical mitotoxic assays, 2) the improvement of drug targeting, 3) the search for drug off-targets, 4) decrease the amount of drug reaching off-targets, 5) engineering of the mitochondrial membrane integrity, and 6) the improvement of mitochondrial bioenergetic parameters. The last two points can be achieved through the co-application of mitochondrial protective agents with appropriate drugs (Olszewska, 2012).

Besides these tailored therapies, a global shield against oxidative stress also would be beneficial. There are other points associated with the complex interactions between respiratory system function, oxidative stressors or cellular signaling pathways that might mediate cellular damage and promote organ failure. Among them, molecules with membrane-regenerative capacity are of importance (Singer, 1999).

1.2. Biological gases

Recent discoveries have radically altered the view of the roles of gases which had previously been considered biologically inert. Signaling functions have been demonstrated for nitric oxide (NO), carbon monoxide (CO) and hydrogen sulfide (H_2S), and research on gas mediators and derivatives has become a topic of interest (Dawson, 1994; Wang, 2003; Ryter, 2004; Wu, 2005; Lamon., 2009; Motterlini, 2010; Rochette, 2013;). In this line, the activity or toxicity of the known gas mediators NO, CO and H_2S is related to their tendency to react with biologically important molecules. It has become increasingly clear that these signaling agents take part in complex pathways, in which they are able to regulate numerous physiological processes, separately, or more often in antagonistic or synergistic ways (Rochette, 2013; Szabó, 2013; Gadhia, 2014).

1.2.1. Methane (CH_4)

Methane CH_4 was earlier commonly thought to be produced in the gastrointestinal (GI) tract exclusively by methanogenic bacterial fermentation, under strictly anaerobic conditions. This notion was challenged when various *in vitro* and *in vivo* studies revealed the possibility of nonmicrobial CH_4 formation in the mitochondria and eukaryote cells in both plants and animals. (Ghyczy 2008b; McLeod, 2008; Bruggemann, 2009; Lenhart, 2009; Messenger, 2009; Wishkerman, 2011). The biological role of methanogenesis in the mammalian physiology is largely unmapped, but it has recently been proposed that CH_4 may be a candidate of the gasotransmitter family (Wang, 2014). CH_4 is part of the omnipresent gaseous environment which maintains aerobic life on Earth. In this gas mixture, CH_4 is intrinsically nontoxic, and widely accepted as knowledge not more than biologically inactive and inert waste. It is a small, uncharged molecule, the most hydrogenated form of carbon. CH_4 is a simple asphyxiant, which means it displaces air and hence O_2 in a restricted area. Tissue hypoxia may occur when the concentration of O_2 in the internal milieu of the body is reduced to 18%.

1.2.2. Bacterial generation of CH_4

On a global scale, an ~2.5-fold increase has been observed in the atmospheric CH_4 concentration since pre-industrial times, and it is therefore considered a significant greenhouse gas of ever greater growing ecological importance (Denman, 2007; Mitchell, 2013). It should be noted that large amounts of CH_4 may be produced by anaerobic fermentation in the mammalian large intestine, where the methanogenic flora produces huge amounts of CH_4 from long-chain alkanes (Zengler, 1999). The microorganisms involved belong in a phylogenetically independent group, the Archaebacteria, a group well distinct from the usual bacteria and the eukaryotes. As an obligate anaerobe, this taxon requires a redox potential of less than -300 mV for life, that a circumstance that is present under water (undersea volcanoes, ricefields and wetlands) or in the GI tract of mammals. Mammalian methanogens can be divided into two groups: H_2/CO_2 and acetate consumers, which are part of a complex microbial consortium, where methanogens obtain substrates from higher levels, from H_2-producers or acetogens (Morris, 2012). Methanogens are compelled to outcompete other microorganisms for the common substrates, such as sulfate-reducing bacteria in the human colon (Strocchi, 1994). Although some of the H_2/CO_2 consumers are also capable of utilizing formate, acetate is consumed by only a limited number of strains. H_2-consuming methanogens are important in maintaining low levels of atmospheric H_2 and in producing

biogas, a possible sustainable alternative for fossil fuel replacement. The methanogenic pathway utilizing CO_2 and H_2 involves 10 methanogen-specific enzymes, which catalyze unique reactions in which several co-enzymes participate (Shima, 2002). The most well-established and common protein of this family is methyl-coenzyme M reductase, which is considered to be the phylogenetic marker of the mammalian methanogenic strains (Friedrich, 2005).

1.2.3. Nonbacterial generation of CH_4

Recent *in vivo* studies have furnished persuasive experimental evidence of the nonbacterial generation of CH_4 in a variety of oxidoreductive stress conditions (Ghyczy, 2001, 2003, 2008; Keppler, 2006; Messenger, 2009). Various study designs have been employed to identify the mechanistic components (**Table 1**) and the results suggest that the release of CH_4 may be a consequence of the production of ROS after transient O_2 deprivation (Ghyczy, 2008a; Keppler, 2008). Hypoxia is inseparable from a mitochondrial dysfunction, and ROS formation is especially pronounced in the inner mitochondrial membrane during the inhibition of cytochrome c oxidase activity (VanUffelen, 1998). More importantly, it has been shown in plants and eukaryotic cells that the CH_4-producing phenomenon can be mimicked by sodium azide (NaN_3) administration (Ghyczy, 2008; Whiskermann, 2011), when selective and stable inhibition of mitochondrial cytochrome c oxidase leads to chemical hypoxia with subsequent energy depletion (Bennett, 1996; Knyihár-Csillik, 1999; Szabados, 2004).

Authors	Origin of CH_4	Cause of CH_4 release
Ghyczy et al., 2003	isolated rat liver mitochondria	treatments with several reducing agents
Keppler et al., 2006	terrestrial plants	leaf injury
Ghyczy et al., 2008	endothelial cell cultures	O_2-glucose deprivation, METC inhibition
McLeod et al., 2008	plant lignin	UV irradiation
Lenhart et al., 2009	fungal cell culture	methionine-rich media
Messenger et al., 2009	plant pectin	UV irradiation
Whiskermann et al., 2011	tobacco and grape cell cultures	NaN_3-induced hypoxia
Althoff et al., 2014	plant methionine	Udenfriend reaction

Table 1. Publications in which nonbacterial CH_4 generation was demonstrated in various experimental conditions.

1.2.4. The biological effects of CH_4

The *in vivo* role of endogenous CH_4 is far from clarified. In humans, the CH_4-producer status (being as >1 part per million (ppm)) in a single breath) has been considered to be involved in various GI disorders, such as chronic constipation or constipation-predominant irritable bowel syndrome (Soares, 2005; Sahakian, 2010). It has been suggested that the presence of methanogenic strains in the large intestine may affect the availability of nutrients for the host. Furthermore, patients with a CH_4/H_2-positive breath test had a significantly higher body-mass index and body fat than the nonproducers (Mathur, 2013). It was also found that *Methanobrevibacter smiithi*, the most prevalent methanogenic strain in the human GI tract, supports obesity in humans (Flourie, 1990). Moreover, it has been demonstrated that 75% of patients with slow colon transit time are CH_4 producers, whereas only 25% of patients with a normal colon transit time are also CH_4 producers (Attaluri, 2010). The contribution of methanogenesis to the molecular mechanism of GI motility is not understood, but it has been shown that exogenous CH_4 can inhibit the contractile activity of the proximal colonic longitudinal muscle by activating the voltage-dependent K^+ channel and increasing the voltage-dependent K^+ current of the colonic smooth muscle cells (Liu, 2013).

1.2.5. CH_4 detection methods

In consequence of its physicochemical properties, CH_4 traverses the mucosa and freely enters the splanchnic microcirculation. It is widely accepted that the bulk of the CH_4 produced is excreted via the lungs, and breath testing has therefore become a tool for the diagnosis of certain GI conditions in humans (Le Marchand, 1992; de Lacy Costello, 2013). Nevertheless, CH_4 is distributed evenly across membrane barriers. The pulmonary route is therefore certainly not exclusive, and the production is reflected not only in the exhaled air, but also in its passage through body surfaces. Indeed, a recent study demonstrated the uniform release of CH_4 through the skin in healthy individuals (Nose, 2005). It follows that determination of the whole-body CH_4 output is required for an assessment of the magnitude of the release or clearance. To date, however, no studies have been reported in which the overall CH_4 generation was investigated or characterized *in vivo*.

In humans, the output of CH_4 or methyl group-containing compounds is usually measured in exhaled air samples by means of gas chromatography (GC) or GC-mass spectrometry (Lewitt, 2006; Ligor, 2008). Nevertheless, traditional methods of breath analysis have limitations and the risk of possible artefacts is high (Yu, 2004). A relatively new option is near-infrared diode laser-based photoacoustic spectroscopy (PAS), which has proven its relevance in life science applications (Cristescu, 2008). PAS is a special mode of optical absorption spectroscopy that is based on the conversion of absorbed light energy into acoustic waves. The technique is based on the thermal expansion of absorbing gas samples: the amplitude of the generated sound is directly proportional to the concentration of the absorbing gas component.

Despite the fact that numerous high-sensitivity PAS-based CH_4 sensors have been reported in the literature, their use for breath analysis is uncommon (Ngai, 2006). PAS provides high selectivity, sensitivity and reliability, and in addition, due to its robust design, it is suitable for measurements outside the laboratory (Bozóki, 2011). Indeed, real-time atmospheric CH_4 measurements have recently been performed with PAS-based sensors (Rocha, 2012; Jahjah, 2014). Nevertheless, near-infrared diode lasers could be effectively used as gas sensors for medical applications due to their excellent stability, long lifetime and low cost.

1.3. L-Alpha-glycerylphosphorylcholine (GPC)

Phosphatidylcholine (PC) is an essential component of biomembranes and endogenous surface-coating substances, and it is well established that the main elements of

ischemia/reperfusion (IR)-induced tissue injuries include lipid peroxidation and the loss of membrane-forming phospholipid bilayers (Volinsky, 2013). Likewise, it has been shown that a reduced PC content of the intestinal mucus plays significant roles in the development of inflammatory bowel diseases (Stremmel, 2012). Interestingly, a number of data suggest that choline-containing phospholipids, including PC, may function as anti-inflammatory substances under highly oxidizing IR conditions. Several studies have indicated that exogenous PC inhibits leukocyte accumulation (Erős, 2009; Hartmann, 2009) and the generation of inflammatory cytokines (Treede, 2009), and dietary PC administration has been demonstrated to provide protection against experimental neuroinflammation, arthritis and pleurisy (Erős, 2009; Hartmann, 2009; Tőkés, 2011) in rodents.

Furthermore, previous results have demonstrated that pretreatment with PC reduces the exhaled CH_4 concentration during an intestinal IR injury (Ghyczy, 2008a). In another *in vitro* study, PC metabolites with an alcoholic moiety in the molecule (i.e. choline, N,N-dimethylethanolamine and N-methylethanolamine) inhibited the ROS-producing activity of isolated leukocytes (Ghyczy, 2008b). Nevertheless, the specific mechanism of action of PC is still not known with certainty, and the question arises as to which of the moieties in the PC molecule are of critical significance in the reduction of the leukocyte responses and pro-inflammatory signal production. The PC molecule is composed of a choline head group and glycerophosphoric acid, with a variety of saturated and unsaturated fatty acids; given their potent bioactions, lipids may be pro-inflammatory or deactivate inflammatory pathway signaling *in vivo* (Bochkov, 2002; Nivala, 2013) and can possibly influence tissue damage. On the other hand, emulsions containing deacylated phospholipid derivatives do not induce endoplasmic reticulum stress or the activation of inflammatory pathway signaling (Nivala, 2013). Furthermore, GPC, a water-soluble, deacylated PC derivative, proved to be effective against lipid peroxidation and loss of the membrane function in oxidoreductive injuries (Onishchenko, 2008). It has been shown to act via cholinergic pathways (Drago, 1992; Sigala, 1992) and has a stimulant effect on the growth hormone response too (Ceda, 1992). GPC has been shown to be protective against membrane oxidation and can ameliorate the membrane function after traumatic injuries (Onischenko, 2008; Kidd, 2009).

II. AIMS AND SCOPES

Our main objective was to investigate nonbacterial biotic methanogenesis and to shed light on the mechanistic details of the reaction.

1. In this framework, our first aim was to design a detection setup to investigate the *in vivo* dynamics of CH_4-producing phenomena specifically and reproducibly. Our primary goal was to determine the whole-body CH_4 release in living, unrestrained small animals.

2. An additional goal was to validate the CH_4 detection system in humans so as to obtain data comparable with those of other studies and methods used for clinical CH_4 breath testing.

3. We hypothesized that a dysfunction of the METC plays distinct roles in the biogenesis of CH_4. We set out to determine the *in vivo* CH_4 production profile after the induction of mitochondrial distress in rodents.

4. We hypothesized that the administration of the potentially methyl-group donor compound GPC might influence the nonbacterial CH_4 release.

5. We also hypothesized that the administration of GPC might afford protection in the form of antigen-independent inflammation accompanying an oxidoreductive imbalance. With this aim, we set out to investigate the effects of GPC in standardized animal models of antigen-independent forms of inflammation evoked by ischemia or irradiation.

III. MATERIALS AND METHODS

3.1.1. Photoacoustic spectroscopy

In clinical practice, CH_4 levels are mostly measured by means of GC, GC-mass spectrometry or He-Ne laser-based technology *(*Levitt, 2006; Ligor, 2008*)*. These methods have major technical limitations, the detection of dynamics is usually not possible and the risk of possible artefacts may be significant *(*Yu, 2004*)*. In our study we employed near-infrared diode laser-based PAS in cooperation with the Department of Optics and Quantum Electronics at the University of Szeged. The light source in this system is a near-infrared diode laser that emits around the CH_4 absorption line at 1650.9 nm with an output power of 15 mW (NTT Electronics, Tokyo, Japan). The narrow line width of the diode laser provides high selectivity; the absorbance of CH_4 is several orders of magnitude greater than that of H_2O, CO_2 or CO at 1.65 μm, the wavelength we used. Cross-sensitivity for common components of breath and ambient air was repeatedly examined, and no measurable instrument response was found for several vol % of CO_2 or H_2O vapor. The instrument was calibrated with various gas mixtures prepared by the dilution of 1 vol % of CH_4 in synthetic

air (Messer, Budapest, Hungary), and proved to have a dynamic range of 4 orders of magnitude; the minimum detectable concentration of the sensor was found to be 0.25 ppm (3σ), with an integration time of 12 s.

3.1.2. Verification by GC

The calibration of the photoacoustic system was verified with a previously calibrated Agilent 6890 GC instrument equipped with a split-splitless inlet HP-Molsieve 5 Å column (30 m * 0.53 mm * 25 μm) and a flame ionization detector. H_2 was used as carrier gas. The inlet parameters were as follows: temperature 150 °C, total flow 40.5 ml min^{-1}. The oven and detector temperatures were 60 °C and 300 °C, respectively. 500 μl of gas mixture was injected manually into the GC instrument with a Hamilton 1750 microsyringe equipped with a pt5 endpoint needle. The analysis time was 1 min per sample. The separation and detection of CH_4 guaranteed the selectivity of the method, and therefore no interference was observed. The measurements were made on the premixed gas standards used for the calibration of the photoacoustic device (1.8-66 ppm). The standard deviation of the GC data was calculated from 4 measurements and proved to be 4.7% on average. The CH_4 content of the ambient air was detected with a signal to noise ratio of 10 to 1. The measurement results of GC and PAS were in good agreement; the average difference was ~1% (n = 8, R^2 = 0.9993).

3.2. Experiments with small animals

The experiments, on male Sprague-Dawley rats (220-300 g (bw)), and SKH-1 hairless mice (32-36 g bw) were performed in accordance with the National Institutes of Health guidelines on the handling and care of experimental animals. All the studies were approved by the Animal Welfare Committee of the University of Szeged.

3.2.1. Whole-body CH_4 analysis setup in rodents

A new, purpose-built device was used to measure the gases emanating from small animals such as rodents as a function of time. Two sampling chambers were constructed for the animals, with regard to their average size and the air volume required for their normal respiration. The chambers and the gas-sampling system were made of glass and stainless steel, respectively, in order to minimize the adverse effects of adsorption-desorption. A 180 cm^3 sampling chamber was prepared for accumulation of the CH_4 emanating from a mouse, and another sampling chamber for measurements on rats (volume: 2510 cm^3) **(Figures 2 and 3).** The chamber consisted of a glass cylinder and two metal plates, a fixed one and a removable one, with a gas outlet port situated on the fixed plate. The chamber included a removable stainless steel grid, ensuring that virtually the whole body surface of the animal remained

uncovered. An animal was laid on the grid and placed into the chamber, and the cylinder tube was then closed with the removable plate.

In the event of continuous sampling, a constant gas concentration is established when the number of gas molecules released from the animal per unit time is equal to the number of gas molecules transferred by the volume of sampled gas per unit time. In other words, if the sampling flow rate is constant, a well-defined CH_4 emission corresponds to a given steady CH_4 concentration. It was found that the CH_4 concentration increased immediately after the animal was placed in the chamber, and a fixed time interval during which there was no gas sampling from the chamber was therefore included to accelerate the building-up of a steady CH_4 concentration. This "accumulation" period was established empirically and optimized for each sampling chamber to abbreviate the procedural time. It was found that 10 min was sufficient for a constant CH_4 concentration to be achieved in the mouse chamber, while in the case of the rat the optimal time for CH_4 "accumulation" was found to be 8 min.

As concerns the determination of the CH_4 concentration of the room air, an initial fluctuation was regularly observed for 1-2 min (depending on the day, the season, the number of persons in the room, etc.) and approximately 5 min was needed to obtain a stable CH_4 signal. During this phase, the chamber was continuously flushed with room air (i.e. the inlet and outlet of the chamber were open) and the baseline CH_4 level was determined for 5 min. The animal was then placed in the glass chamber and the "accumulation" period was started. After the "accumulation" period, the membrane pump began to draw gas through the photoacoustic cell at a flow rate of 4.5 cm^3 min^{-1}; the plate with which the chamber was closed allowed the sampled gas volume to be replaced with ambient air. In each measurement, a plateau level was reached after 6-8 min, and thereafter remained steady until the end of the 10-min observation period. The whole-body emissions were calculated without the background CH_4 level, and the values were referred to the body surface area of the animals. Figure 4 shows a typical measurement curve in a mouse. If the 4.5 cm^3 gas sample sampled in 1 min contains 1 ppm CH_4 (without the background CH_4 level), then the CH_4 emission is 2.9 10^{-9} g min^{-1}. In order to simplify evaluations, the CH_4 release is given in ppm/(cm^2 10^3).

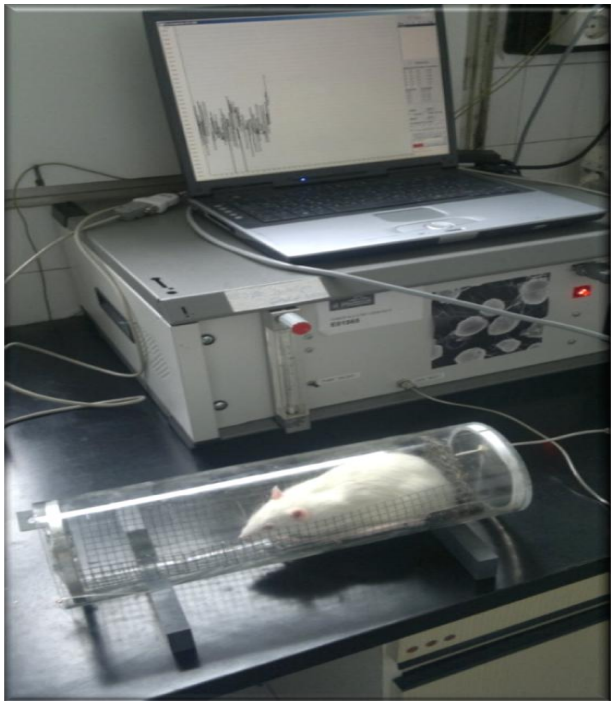

Figure 2. Rats were kept in a hermetically closed chamber, while the air was drawn by a pump directly into the photoacoustic chamber.

Figure 3. Mice were kept in a hermetically closed chamber, while the air was drawn by a pump directly into the photoacoustic chamber.

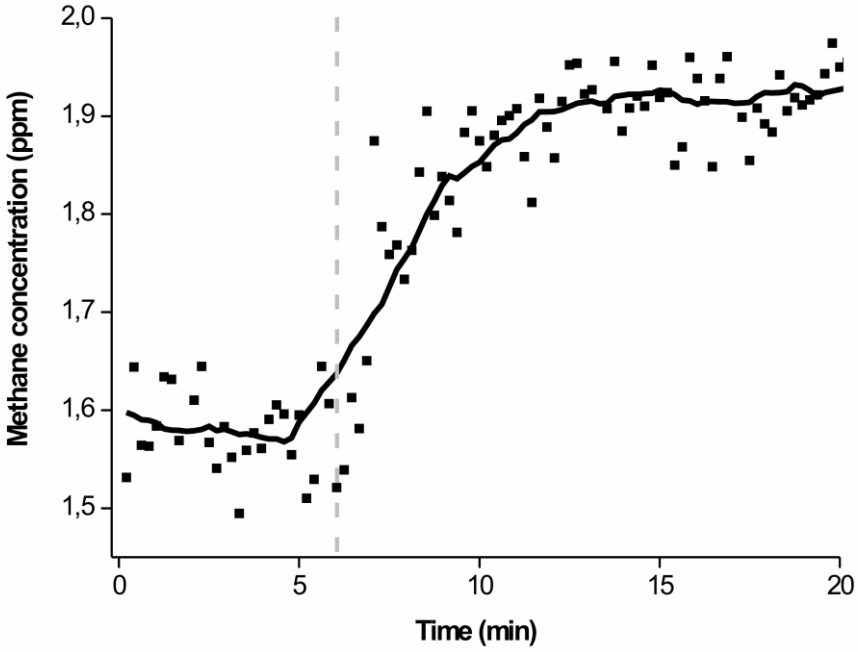

Figure 4. Control CH_4 measurement in a mouse. For several min, the CH_4 concentration of the room air was measured; and the vertical dashed line indicates the time when the gas flow from the chamber started. The solid gray curve shows the moving the average over 20 points. Baseline measurements are not shown for the total "accumulation" time (which was 10 min).

3.3. Human study, participants and protocol

CH_4 measurements in humans were performed at preset times (the same hour of the day) just before the first meal. The participants were subgrouped as males (n = 44) or females (n = 39), children (aged ≤ 20 years; n = 42) or adults (aged ≥ 21 years; n = 41). The CH_4 concentration of the exhaled air was measured. Participants were considered to be CH_4 producers if the exhaled CH_4 concentration exceeded 1 ppm.

3.3.1. Sampling for CH_4 measurements

The CH_4 concentration of the room air was determined and used as baseline in the calculations of the CH_4 emission. Afterwards, the subject was asked to breathe normally and the expired air was directed into a glass flask (volume: 200 cm^3) (**Figure 5**). The optimal time for the attainment of a steady CH_4 concentration at a flow rate of 30 cm^3 min^{-1} proved to be between 1 and 3 min.

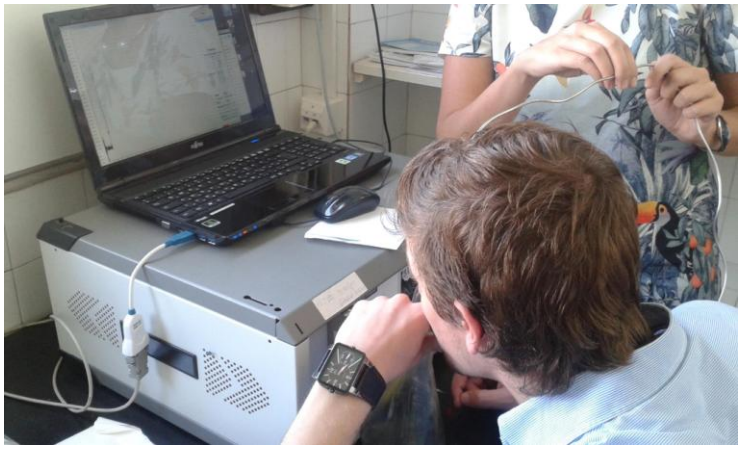

Figure 5. The human volunteers were asked to breathe normally into a glass flask via a glass pipe, while the air was drawn by a pump directly into the photoacoustic chamber.

3.4. Induction of a mitochondrial dysfunction in rodents

3.4.1. Experimental protocol 1. Chronic NaN_3 treatment of rats

35 rats were randomly allocated into 5 groups. Group 1 (n = 7) served as sham-operated, non-treated controls; in Group 2 (n = 7), the rats were treated with a dose of 14 mg kg^{-1} day^{-1} subcutaneously (sc) NaN_3 (Sigma-Aldrich, Munich, Germany) for 8 days. This dose has been reported to produce a nonlethal inflammatory response in rodents. The significant inhibition of cytochrome c oxidase activity by treatment with NaN_3 was demonstrated in pilot experiments by fluorometric analysis of liver samples. In Group 3 (n = 7), the NaN_3 treatment (14 mg kg^{-1} day^{-1} sc for 8 days) was supplemented with parallel, oral GPC treatment (Lipoid GmbH, Ludwigshafen, Germany, 50 mg kg^{-1} day^{-1}) in daily gavages for 8 days. In Group 4 (n = 7), the animals were treated orally with the antibiotic rifaximin (10 mg kg^{-1} day^{-1}; Alfa Wasserman, West Caldwell, NJ, USA) for 11 days, the first dose being administered 3 days before the start of NaN_3 treatment (14 mg kg^{-1} day^{-1} for 8 days). This procedure resembles the clinical practice of targeting the GI bacterial flora; the rifaximin dose was chosen with regard to the overall minimal inhibitory concentration (25 μg ml^{-1}) at which 50% of the strains are inhibited (Finegold, 2009). Group 5 (n = 7) served as a control group, in which the animals received only oral rifaximin (10 mg kg^{-1} day^{-1} orally for 11 days). Whole-body CH_4 emission was measured every second days over the 8 day in the various groups, and the animals were then anesthetized with 5% chloral hydrate (375 mg kg^{-1}) in order to carry out the intravital examinations. Tissue biopsies were subsequently taken to determine certain biochemical parameters; the samples were stored at -70 ^{o}C until the measurements.

3.4.2. Experimental protocol 2. Endotoxin challenge in mice

In this study, 24 SKH-1 hairless mice mice were randomly allocated into 3 groups. Group 1 (n = 8) served as untreated controls. The animals in Group 2 (n = 8) underwent intestinal flora eradication: 10 mg kg^{-1} of rifaximin was administered orally via gavage. This treatment was repeated 2 days later. After another period of 2 days, the CH_4 emission of the animals was determined. In Group 3 (n = 8) 5 mg kg^{-1} ip lipopolysaccharide (LPS) was administered and the whole-body CH_4 release was recorded 3 h later.

3.4.3. Experimental protocol 3. Intestinal IR in rats

32 rats were randomly allocated into four groups (n = 8 each): a control, sham-operated group, a group that participated in intestinal IR, and groups that took part in IR with GPC pretreatment (GPC + IR) or in IR with GPC post-treatment (IR + GPC). The GPC (MW: 257.2, Lipoid GmbH, Ludwigshafen, Germany) was administered intravenously (iv) in a dose of 16.56 mg kg^{-1} bw, as a 0.064 mM solution in 0.5 ml sterile saline. These dosage conditions were based on the data of previous investigations with PC. This dose was equimolar with the effective, anti-inflammatory dose of PC (MW: 785; 0.064 mM, 50 mg kg^{-1} bw, iv) in rodents (Varga et al., 2006; Gera et al., 2007). The GPC pre- or post-treatment was applied once, either directly before the ischemic period or immediately after the ischemia, before the start of reperfusion. The animals were anesthetized with sodium pentobarbital (50 mg kg^{-1} bw ip) and placed in a supine position on a heating pad. Tracheostomy was performed to facilitate spontaneous breathing, and the right jugular vein was cannulated with polyethylene (PE50) tubing for fluid administration and Ringer's lactate infusion (10 ml kg^{-1} h^{-1}) during the experiments. The right common carotid artery was cannulated with PE50 tubing for mean arterial pressure and heart rate measurements. After midline laparotomy, the animals in the IR, GPC + IR and IR + GPC groups were subjected to 45 min ischaemia by occlusion of the superior mesenteric artery (SMA) with an atraumatic vascular clamp. 45-min after the start of the ischemic insult, the vascular clamp was removed and the intestine was reperfused. The SMA blood flow was measured continuously with an ultrasonic flowmeter (Transonic Systems Inc., Ithaca, NY, U.S.A.) placed around the mesenteric artery. The abdomen was temporarily closed and the intestine was reperfused for 180 min. In the sham-operated control group, the animals were treated in an identical manner except that they did not undergo clamping of the artery. After 180 min of reperfusion, tissue samples were taken from the liver to determine the ATP content.

3.4.4. Experimental protocol 4. Irradiation injury in rats

18 rats were anesthetized with 5% chloral hydrate solution and placed in a supine position on a heating pad. The right jugular vein was cannulated with polyethylene (PE50) tubing for the maintenance of anesthesia (5% chloral hydrate) and for treatment. Group 1 (n = 6), which served as nontreated controls, received sterile saline (0.5 ml iv). Computed tomography (CT)-based (Emotion 6-Siemens AG, Erlangen, Germany) three-dimensional conformal treatment planning was performed with the XIO™ (CMS, ELEKTA, Stockholm, Sweden) treatment planning system. The hippocampus was delineated on each slice on CT images acquired in the treatment position. Two opposed isocentric lateral circle fields 1 cm in diameter were planned, resulting in a homogeneous dose distribution in the target. The field profile and output factor of the custom-made collimator were measured by using film dosimetry and a pinpoint ionization chamber. For the irradiation, the animals were laid on a special positioning scaffold (resembling a bunk-bed, 3 rats at a time). Group 2 (n = 6) and Group 3 (n = 6) were subjected to cobalt 60 teletherapy (Terragam K01, SKODA UJP, Prague, Czech Republic) of the hippocampus in both hemispheres: 40 Gy (1 Gy/2.25 min), from two opposed lateral fields. The dosage level selected for the study protocol was based on the data of previously published investigations (Münter et al. 1999; Karger et al. 2002); biological responses to different single doses were also defined in pilot experiments (data not shown). It should be added that the radiotolerance of the rat brain is different from that of the human brain, and structural changes, including decreases in cell number and demyelination, can be expected in the 50-100 Gy dose range (Münter, 1999). Prior to the start of radiation, portal imaging with the gamma ray of the Cobalt unit was performed for field verification. Additionally, Group 3 received GPC (Lipoid GmbH, Ludwigshafen, Germany; 50 mg kg^{-1} bw, dissolved in 0.5 ml sterile saline, iv) 5 min before the start of irradiation. Three h after the completion of irradiation, the animals were killed by decapitation and additional liver samples were immediately taken to determine tissue ATP changes.

3.5. Biochemical measurements

3.5.1. ATP measurements

A sample was taken from the liver, cooled in liquid nitrogen, and stored at -70 ^{o}C. Afterwards, it was subsequently weighed, placed into a 3-fold volume of trichloroacetic acid (6% w/v), homogenized for 1 min, and centrifuged at 5000 g. After adjustment of the pH to 6.0 with saturated K_2CO_3 solution, the reaction mixtures were prepared by the addition of 100 µl of ATP assay mix (containing firefly luciferase, luciferin, $MgSO_4$,

ethylenediaminetetraacetic acid (EDTA), dithiotreitol (DTT) and bovine serum albumin in a Tricine buffer; Sigma-Aldrich GmbH, Munich, Germany) to 100 µl of 5-fold diluted sample. The ATP determinations were based on the measurement of luciferase chemiluminescence, using a luminometer (LUMAT LB 9507, Berthold Technologies, GmbH, Bad Wilbad, Germany). ATP levels were calculated with the aid of a standard ATP calibration curve (Sigma-Aldrich GmbH, Germany). The data were referred to the sample weights.

3.5.2. Intestinal xanthine oxidoreductase (XOR) activity

Small intestinal biopsies kept on ice were homogenized in phosphate buffer (pH 7.4) containing 50 mM Tris-HCl (Reanal, Budapest, Hungary), 0.1 mM EDTA, 0.5 mM DTT, 1 mM phenylmethylsulfonyl fluoride (PMSF), 10 µg ml^{-1} soybean trypsin inhibitor and 10 µg ml^{-1} leupeptin. The homogenate was centrifuged at 4 ^{o}C for 20 min at 24, 000 g and the supernatant was loaded into centrifugal concentrator tubes. The activity of XOR was determined in the ultrafiltered supernatant by fluorometric kinetic assay.

3.5.3. Intestinal and lung tissue myeloperoxidase (MPO) activity

The activity of MPO, a marker of polymorphonuclear (PMN) leukocyte activation, was determined in ileal and lung biopsies. Samples were homogenized with Tris-HCl buffer (0.1 M, pH 7.4) containing 0.1 mM PMSF to block tissue proteases, and then centrifuged at 4 ^{o}C for 20 min at 24, 000 g. The enzyme reaction mixture containing 50 mM K_3PO_4 buffer (pH 6.0), 2 mM 3,3' 5,5'-tetramethylbenzidine (dissolved in dimethyl sulfoxide (DMSO)) and 100 µl of homogenate supernatant was incubated for 5 min at 37 ^{o}C. The reaction was started with 0.6 mM hydrogen peroxide (H_2O_2) dissolved in 0.75 ml of K_3PO_4 buffer) and was stopped after 5 min with 0.2 ml of H_2SO_4 (2 M) and the H_2O_2-dependent oxidation of tetramethylbenzidine was detected spectrophotometrically at 450 nm (UV-1601 spectrophotometer, Shimadzu, Kyoto, Japan). MPO levels were calculated via a calibration curve prepared with standard MPO (Sigma-Aldrich GmbH, Munich, Germany). The data were referred to the protein content.

3.5.4. Intestinal superoxide ($O_2^{\cdot -}$:) production

The level of $O_2^{\cdot -}$: production in freshly minced intestinal biopsy samples was assessed by a lucigenin-enhanced chemiluminescence assay (Ferdinandy, 2000). Briefly, ~25 mg of intestinal tissue was placed in 1 ml of Dulbecco's solution (pH 7.4) containing 5 µM lucigenin. The manipulations were performed without external light 2 min after dark adaptation. Chemiluminescence was measured at room temperature in a liquid scintillation counter by using a single active photomultiplier positioned in out-of-coincidence mode, in the

presence or absence of the $O_2^{\cdot -}$: scavenger nitroblue tetrazolium (NBT; 20 µl). NBT-inhibited chemiluminescence was considered an index of intestinal $O_2^{\cdot -}$: generation.

3.6. Tissue injury analysis

3.6.1. Intravital videomicroscopy (IVM)

The microcirculation of the liver surface was visualized by means of IVM, using a Zeiss Axiotech Vario 100HD microscope (100 W HBO mercury lamp, Acroplan 20x water immersion objective). Fluorescein isothiocyanate FITC; Sigma Chemicals, St. Louis, MO, USA, 0.2 ml iv) was used for the ex-vivo labeling of erythrocytes, and rhodamine-6G (Sigma, St. Louis, MO, USA, 0.2%, 0.1 ml i.v.) for the staining of PMN leukocytes. The microscopic images were recorded with a charge-coupled device videocamera (AVT HORN-BC 12, Horn Imaging, Aalen, Germany) attached to an S-VHS videorecorder (Panasonic AG-MD 830, Yokohama, Japan) and a personal computer.

3.6.2. Video analysis

Quantitative assessment of the microcirculatory parameters was performed off-line by frame-to-frame analysis of the videotaped images, using image analysis software (IVM, Pictron Ltd., Budapest, Hungary). The red blood cell velocity (RBCV, µm s^{-1}) was measured in 5 separate fields in 5 sinusoids. The functional capillary density (FCD) was defined as the total length of red blood cell-perfused capillaries per observation area (cm cm^{-2}). Leukocyte-endothelial cell interactions were analyzed within 5 central venules of the liver (diameter between 11 and 20 µm) per animal. Adherent leukocytes (stickers) were defined in each vessel segment as cells that did not move or detach from the endothelial lining within an observation period of 30 s, and are given as the number of cells per mm^2 of endothelial surface.

3.6.3. In vivo histology

The dynamic structural changes of the liver were investigated by real-time laser scanning confocal endomicroscopy with an excitation wavelength of 488 nm, the emission being detected at 505 to 585 nm (FIVE1, Optiscan Pty Ltd, Notting Hill, Australia). The chosen areas were scanned in a raster pattern to construct a transverse optical section (1 scan per image, 1024 x 512 pixels and 475 x 475 µm per image). The optical slice thickness was 7 µm; the lateral and axial resolution was 0.7 µm. The liver architecture was examined *in vivo* following topical application of the fluorescent dye acridine orange (Sigma-Aldrich Inc, St. Louis, Missouri, USA). The objective of the device was placed onto the liver surface, and confocal imaging was performed 5 min after dye administration. 30-50 pictures were stored in

each experiment. The thickness of the sinusoids was quantified by image analysis; the qualitative lobular changes were analyzed by using a semiquantitative scoring system. The grading was performed with three criteria: the structural changes of the sinusoids (score 0 = normal; 1 = dye extravasation, but the vessel structure is still recognizable; 2 = destruction, the vessel structure is unrecognizable), edema (score 0 = no edema; 1 = moderate epithelial swelling; 2 = severe edema), and the hepatocyte cell outlines (score 0 = normal, well-defined outlines; 1 = blurred outlines; 2 = lack of normal cellular contours).

3.7. Statistical analysis

Data analysis was performed with a statistical software package (SigmaStat for Windows, Jandel Scientific, Erkrath, Germany). Due to the non-Gaussian data distribution, nonparametric methods were used in the animal experiments, and thus Friedman repeated measures analysis of variance on ranks was applied within groups. Time-dependent differences from the baseline (0 min) for each group were assessed by Dunn's method, and differences between groups were analyzed with Kruskal-Wallis one-way analysis of variance on ranks, followed by Dunn's method for pairwise multiple comparisons. The Mann-Whitney U-probe was applied to assess the differences between human samples. In the Figures, median values and 75^{th} and 25^{th} percentiles are given. p values < 0.05 were considered significant.

IV. RESULTS

4.1. Whole-body CH_4 release after mitochondrial distress

4.1.1. CH_4 release in control and NaN_3-treated rats

We first estimated the average CH_4 emission of a group of healthy rats during a whole-day interval in order to observe the possible fluctuations. We took the whole-body CH_4 production data of 4 rats every second hour; the amount of gas generated within 24 hours was between 1.007 dppm/1000 dm^2 and 1.394 dppm/1000 dm^2 within 24 hours (data not shown).

We then performed repeated analyses at two-days intervals to follow the CH_4 profile of the rats (**Figure 6**). Chronic NaN_3 administration significantly increased the whole-body generation of CH_4 by day 3 of treatment (M: 2.082 dppm/1000 dm^2; p25: 1.992 dppm/1000 dm^2; p75: 2.277 dppm/1000 dm^2), and the higher CH_4 output persisted until the end of the experiments (day 8: M: 2.974 dppm/1000 dm^2; p25: 2.630dppm/1000 dm^2; p75: 3.362 dppm/1000 dm^2).

A statistically significant increase in CH_4 release was observed on day 8 in the antibiotic-treated animals subjected to the NaN_3 challenge (M: 2.224 dppm/1000 dm^2; p25:

1.528 dppm/1000 dm^2; p75: 2.346 dppm/1000 dm^2), whereas no elevation was noted in the sham-operated (M: 1.337 dppm/1000 dm^2; p25: 1.078 dppm/1000 dm^2; p75: 1.598 dppm/1000 dm^2) or antibiotic-treated (M: 1.598 dppm/1000 dm^2; p25: 0.938 dppm/1000 dm^2; p75: 1.673 dppm/1000 dm^2) control groups.

In the GPC + NaN_3-treated group (M: 1.11 dppm/1000 dm^2; p25: 0.83 dppm/1000 dm^2; p75: 1.437 dppm/1000 dm^2) a significant CH_4 level elevation was not demonstrated relative to the matching controls. The elimination of the intestinal bacteria led to a considerable decrease in CH_4 emission, but it remained measurable (M: 1.135 dppm/1000 dm^2; p25: 0.848 dppm/1000 dm^2; p75: 1.312 dppm/1000 dm^2) and by day 8 the level was significantly higher in the animals subjected to the NaN_3 challenge than in the control group.

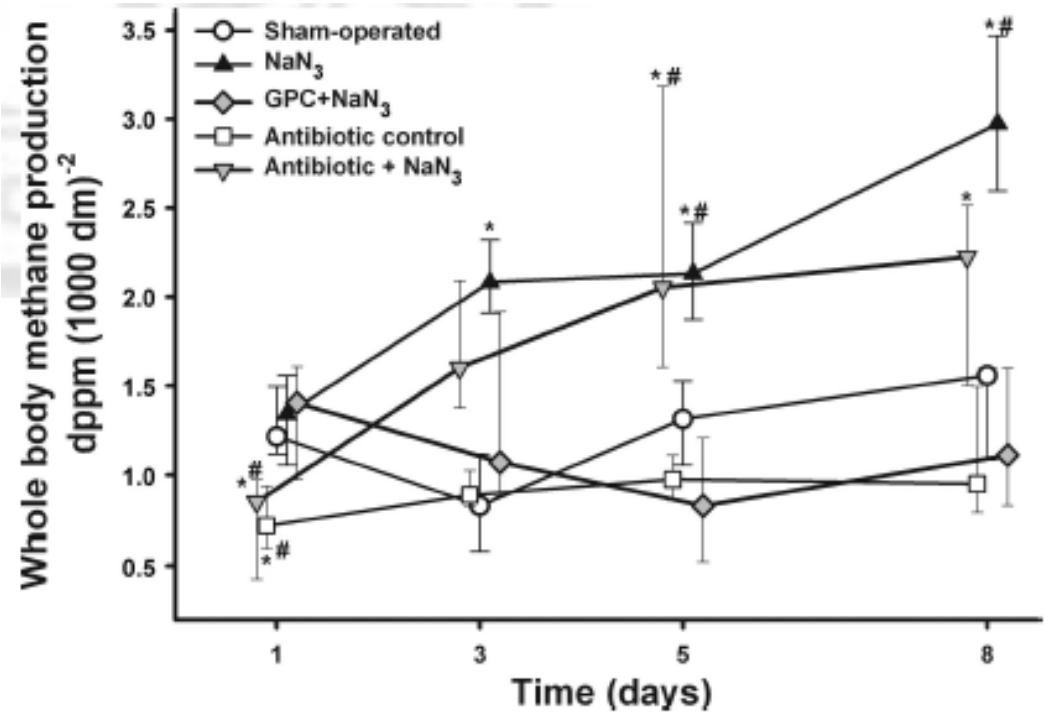

Figure 6. Whole-body CH_4 production on days 1, 3, 5 and 8 of the investigation. The empty circles with a continuous line relate to the sham-operated group, the black triangles with a continuous line to the NaN_3-treated group, the gray diamonds with a continuous line to the GPC-treated NaN_3 group, the empty squares with a continuous line to the antibiotic-gavaged control group, and the gray inverted triangles with a continuous line to the antibiotic-gavaged NaN_3-treated group. During the first measurement, all the rats were untreated, except for the antibiotic-treated group, which had been pretreated for 3 days. Median values and 75^{th} and 25^{th} percentiles are given. $^{*}p < 0.05$ vs sham-operated, or antibiotic-treated control; $^{\#}$ $p < 0.05$ vs the GPC + NaN_3-treated group.

4.1.2. CH_4 release in control and LPS-treated mice

A measurable CH_4 release was observed in each animal in the control group of mice (M: 3.25 ppm/cm^2 10^3; p25: 3.00 ppm/cm^2 10^3; p75: 3.89 ppm/cm^2 10^3) (**Figure 7**). The antibiotic treatment led to a significantly lower, but still measurable CH_4 emission (M: 1.71 ppm/cm^2 10^3; p25: 1.50 ppm/cm^2 10^3; p75: 2.11 ppm/cm^2 10^3). However, the application of LPS increased the CH_4 production considerably (M: 4.53 ppm/cm^2 10^3; p25: 4.37 ppm/cm^2 10^3; p75: 5.38 ppm/cm^2 10^3).

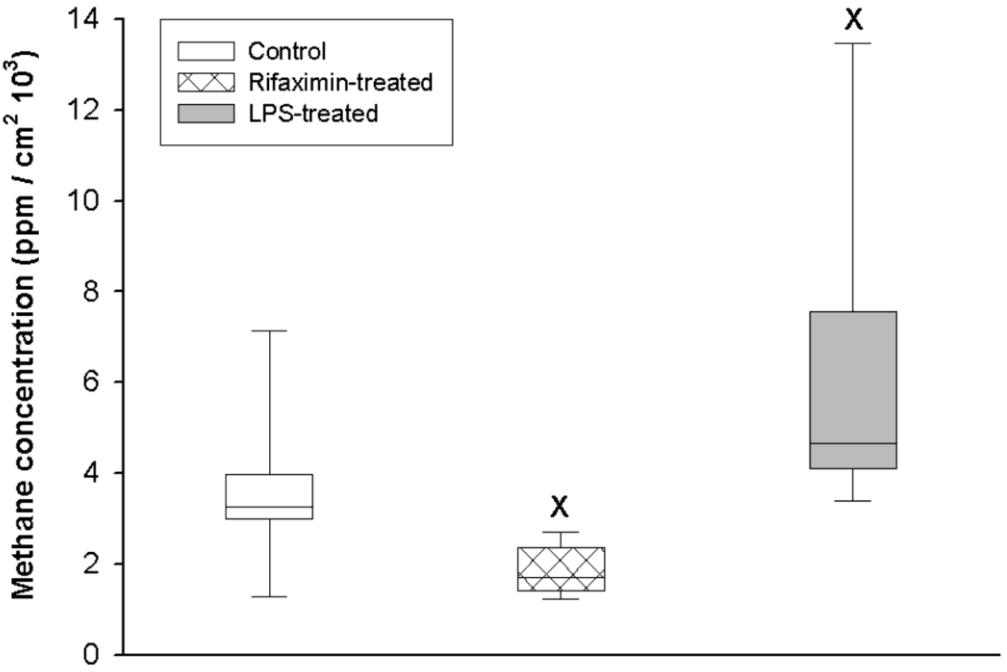

Figure 7. Whole-body CH_4 production in mice. White box: untreated control group, hatched box: rifaximin-treated group, gray box: LPS-treated group. Median values and 75th and 25th percentiles are given. ^{x} $p < 0.05$ vs control.

4.2. Human measurements

4.2.1. CH_4 concentration of the exhaled breath of healthy humans

The determined range was found to be between 0 and 36.9 ppm. 21% of the population proved to be CH_4 producers. There was no difference between the males and females in cumulative CH_4 production (**Figure 8**) ($p = 0.831$). The amount of CH_4 produced was higher among the adults than among the children (**Figure 9**) ($p = 0.079$).

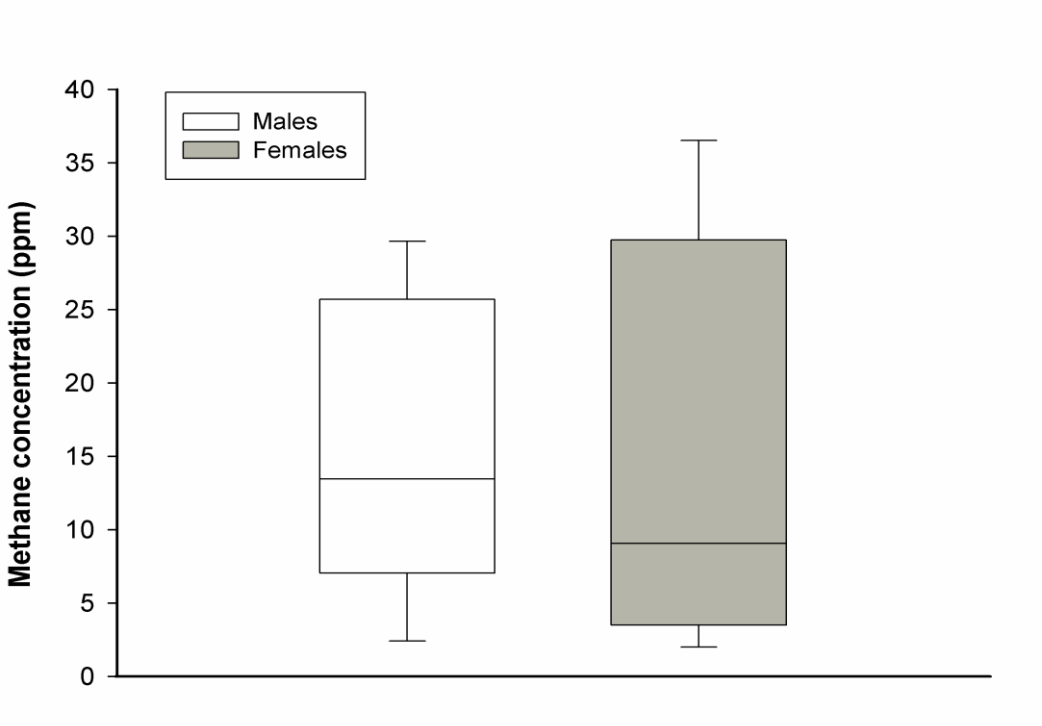

Figure 8. Exhaled CH_4 concentrations in humans. The white boxes show data for adult males, while the gray boxes show data for adult females. Median values and 75th and 25th percentiles are given.

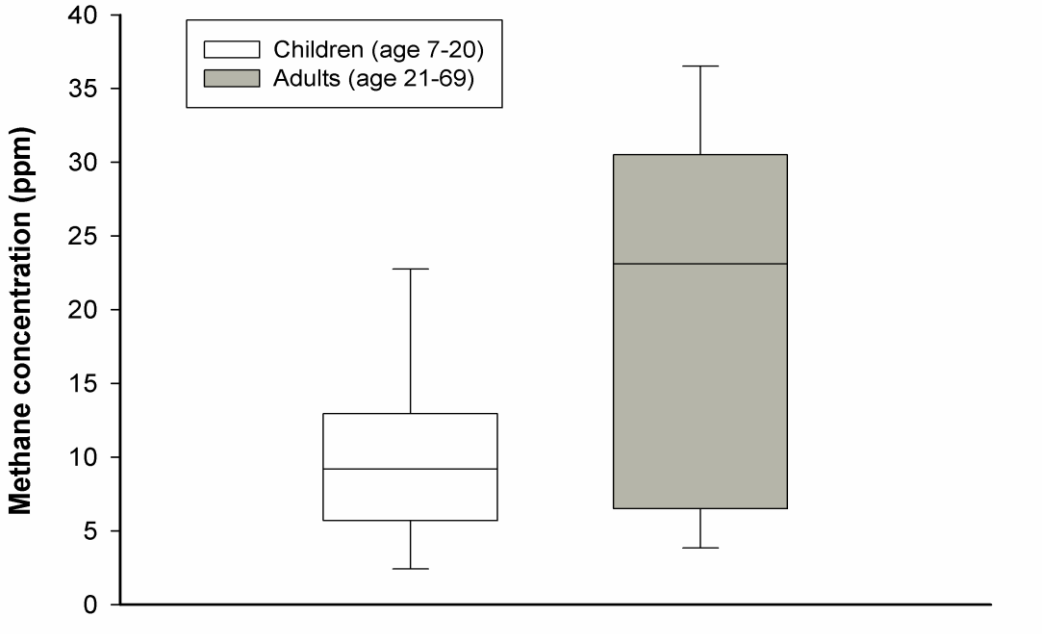

Figure 9. Exhaled CH_4 concentrations in humans. The white boxes show data for children, while the gray boxes show data for adults overall. Median values and 75th and 25th percentiles are given.

4.3. The effects of GPC on the consequences of a NaN_3-induced mitochondrial dysfunction

4.3.1. Liver ATP levels

In order to establish whether NaN_3 influences the mitochondrial function, we quantified the liver ATP production on day 8 of the chronic challenge. The results indicated a significant ATP depletion in Group 2 (M: 0.122 nmol ml^{-1} mg^{-1}; p25: 0.089 nmol ml^{-1} mg^{-1}; p75: 0.189 nmol ml^{-1} mg^{-1}) in comparison with the sham-operated group (**Figure 10**). The ATP level in the liver of the GPC-gavaged group was higher, but the increase was not significant statistically (M: 0.199 nmol ml^{-1} mg^{-1}; p25: 0.182 nmol ml^{-1} mg^{-1}; p75: 0.222 nmol ml^{-1} mg^{-1}) as compared with either the NaN_3-treated or the antibiotic-gavaged + NaN_3-treated group. The GPC-treated animals produced a similar amount of ATP as observed in the control groups.

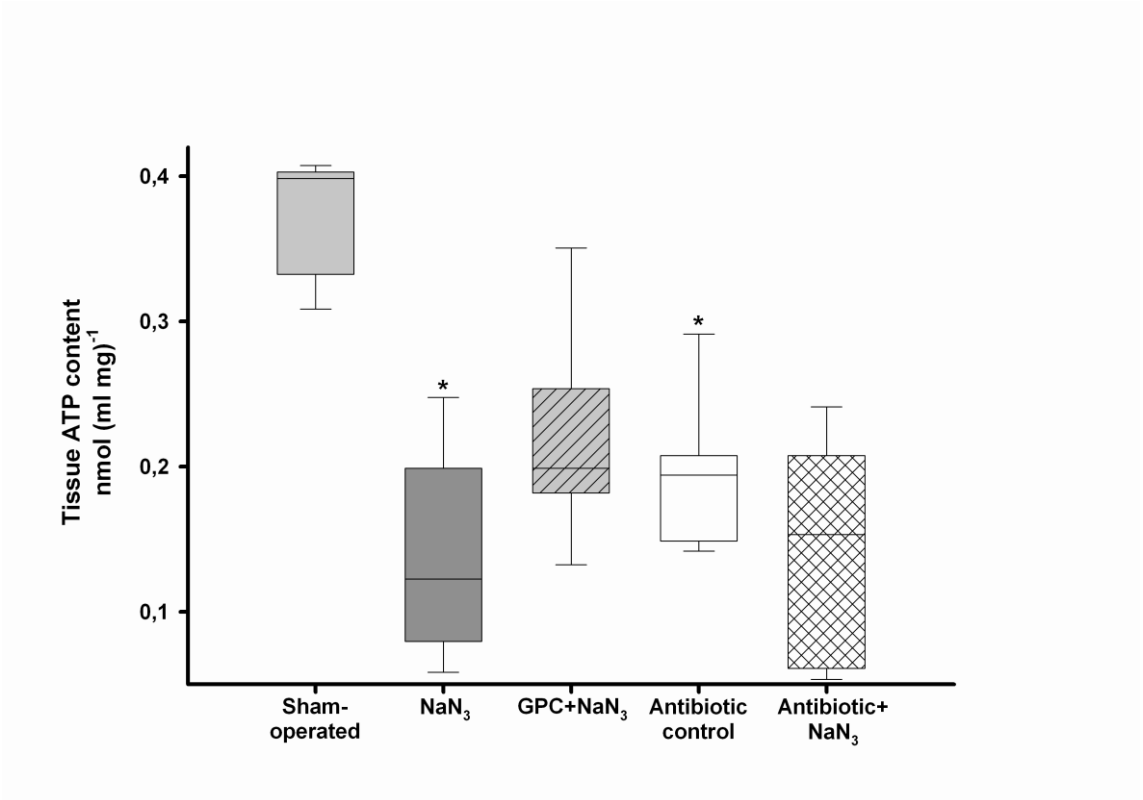

Figure 10. Tissue ATP contents of liver samples. The light-gray box plot relates to the sham-operated group, the dark-gray box plot to the NaN_3-treated group, the striped light-gray box plot to the GPC-treated NaN_3 group, the white box plot to the antibiotic-gavaged control group, and the checked white box plot to the antibiotic-gavaged NaN_3-treated group. Median values and 75^{th} and 25^{th} percentiles are given. $^{*}p < 0.05$ vs the sham-operated, or antibiotic-treated control.

4.3.2. XOR activity in the small intestine after NaN_3 administration

The activation of XOR during hypoxia or IR events leads to the production of high amounts of ROS. Thus, the small intestinal XOR was chosen as a further endpoint via which to characterize the inflammatory potential of NaN_3 administration. By day 8 of the experiments, a significantly higher ileal XOR activity was noted in the animals subjected to the NaN_3 challenge (M: 316.2 pmol min^{-1} mg^{-1}; p25: 240.9 pmol min^{-1} mg^{-1}; p75: 535.4 pmol min^{-1} mg^{-1}) as compared with the GPC-treated Group 3 (M: 153.9 pmol min^{-1} mg^{-1}; p25: 121 pmol min^{-1} mg^{-1}; p75: 198.5 pmol min^{-1} mg^{-1}) and Group 4 (M: 216.9 pmol min^{-1} mg^{-1}; p25: 187.1 pmol min^{-1} mg^{-1}; p75: 243.5 pmol min^{-1} mg^{-1}) (**Figure 11**). The increase was statistically not significant in the antibiotic + NaN_3-treated Group 5 in comparison with the matching control.

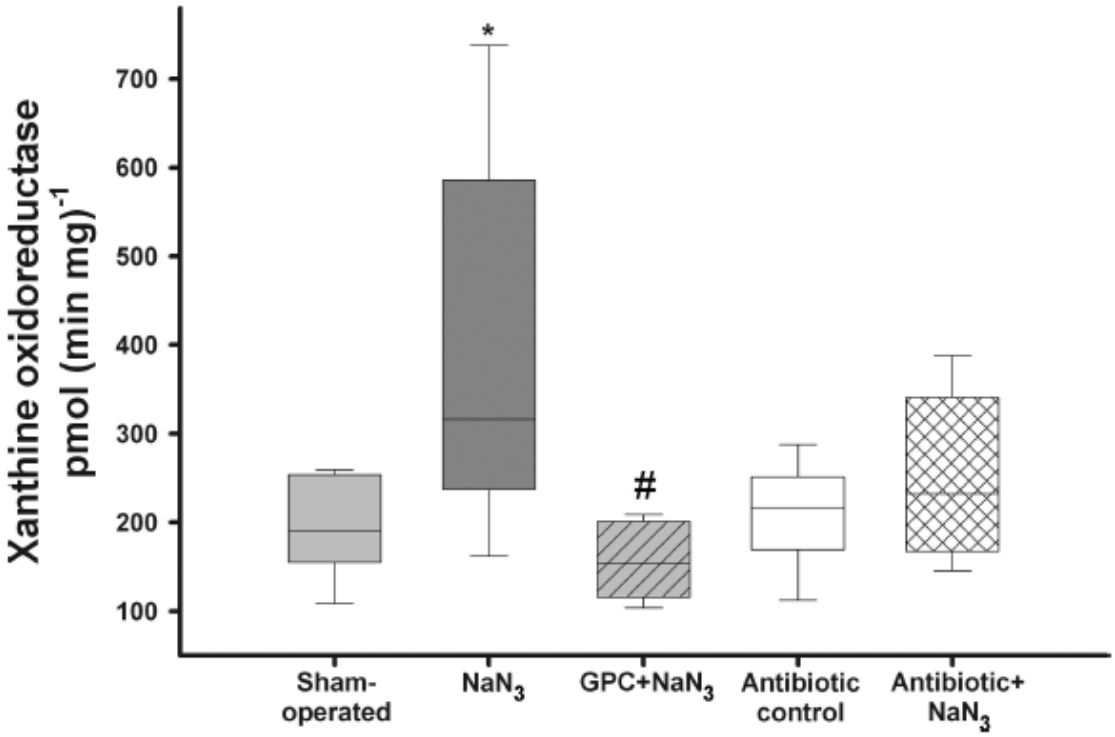

Figure 11. Tissue XOR activities of the ileal samples. The light-gray box plot relates to the sham-operated group, the dark-gray box plot to the NaN_3-treated group, the striped light-gray box plot to the GPC-treated NaN_3 group, the white box plot to the antibiotic-gavaged control group, and the checked white box plot to the antibiotic-gavaged NaN_3-treated group. Median values and 75^{th} and 25^{th} percentiles are given, $^{*}p < 0.05$ vs sham-operated, or antibiotic-treated control; $^{\#}p < 0.05$ vs GPC + NaN_3-treated group.

4.3.3. MPO activities of the ileum and the lung

The MPO produced by the activated leukocytes was chosen as an indicator of the general inflammatory profile of the rat tissues. As reflected in **Figure 13**, we observed statistically significant increases in lung MPO in the NaN_3-treated Group 2 (M: 570 pmol min^{-1} mg^{-1}; p25: 544.5 pmol min^{-1} mg^{-1}; p75: 805.5 pmol min^{-1} mg^{-1}) and the antibiotic + NaN_3-treated Group 5 (M: 501.7 pmol min^{-1} mg^{-1}; p25: 383.8 pmol min^{-1} $mg^{-1;}$ p75: 1268.5 pmol min^{-1} mg^{-1}) as compared with the sham-operated control or the GPC-supplemented group (M: 300.5 pmol min^{-1} mg^{-1}; p25: 277.3 pmol min^{-1} mg^{-1}; p75: 305.9 pmol min^{-1} mg^{-1}). In the GPC-gavaged group, the MPO activity was even lower than in the control groups.

Quantification of the MPO activity in the ileum revealed significant elevations in the NaN_3-treated animals (M: 1271.5 pmol min^{-1} mg^{-1}; p25: 1154.4 pmol min^{-1} mg^{-1}; p75: 1366.5 pmol min^{-1} mg^{-1}) and the antibiotic-gavaged NaN_3-treated groups (M: 1274.6 pmol min m^{-1} mg^{-1}; p25: 782.3 pmol min^{-1} mg^{-1}; p75: 1828.6 pmol min^{-1} mg^{-1}) (**Figure 12**). GPC supplementation resulted in a significantly lower MPO activity (M: 914.5 pmol min^{-1} mg^{-1}; p25: 783.3 pmol min^{-1} mg^{-1}; p75: 944.9 pmol min^{-1} mg^{-1}) and the data did not differ from those for the sham-operated group (M: 818.3 pmol min^{-1} mg^{-1}; p25: 801.7 pmol min^{-1} mg^{-1}; p75: 866.5 pmol min^{-1} mg^{-1}).

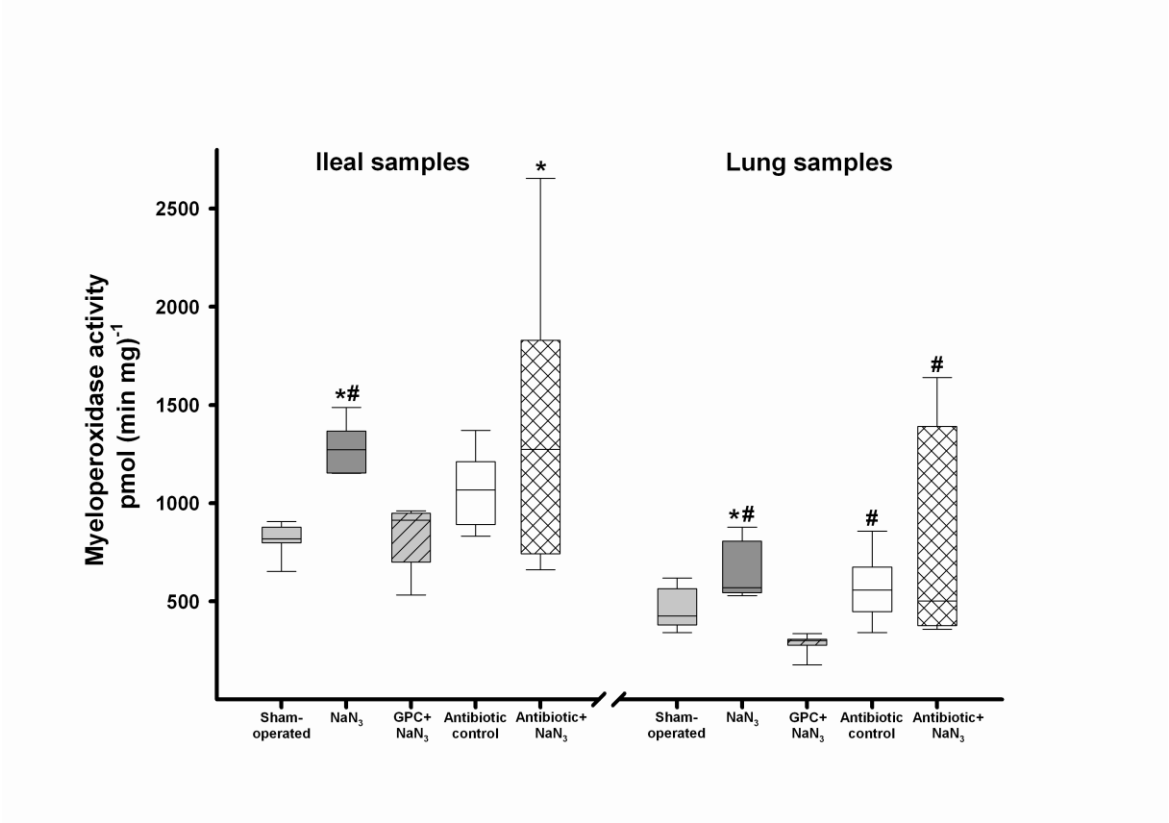

Figure 12. Tissue MPO activities of the ileal and lung biopsy samples. The light-gray box plot relates to the sham-operated group, the dark-gray box plot to the NaN_3-treated group, the striped light-gray box plot to the GPC-treated NaN_3 group, the white box plot to the antibiotic-gavaged control group, and the checked white box plot to the antibiotic-gavaged NaN_3-treated group. Median values and 75th and 25th percentiles are given. $p < 0.05$ was considered statistically significant. $^{*}p < 0.05$ vs sham-operated, or antibiotic-treated control; $^{\#}p < 0.05$ vs the GPC+NaN_3-treated group.

4.3.4. Liver microcirculation during chemical hypoxia

The hepatic microcirculation is well known to be particularly sensitive to inflammatory damage and chemical hypoxia, and the NaN_3-induced changes in RBCV and FCD were therefore monitored (**Figure 13**). In Group 2, the RBCV in the sinusoids was very low (M: 314.5 μm s^{-1}; p25: 290 μm s^{-1}; p75: 348 μm s^{-1}) relative to the sham-operated value (M: 812 μm s^{-1}; p25: 777 μm s^{-1}; p75: 839 μm s^{-1}). After GPC administration, the RBCV increased significantly, but did not reach the control level (M: 444 μm s^{-1}; p25: 408 μm s^{-1}; p75: 616.5 μm s^{-1}). A similar tendency was observed in the antibiotic + NaN_3-treated Group 5. No differences in FCD were found between the groups (data not shown).

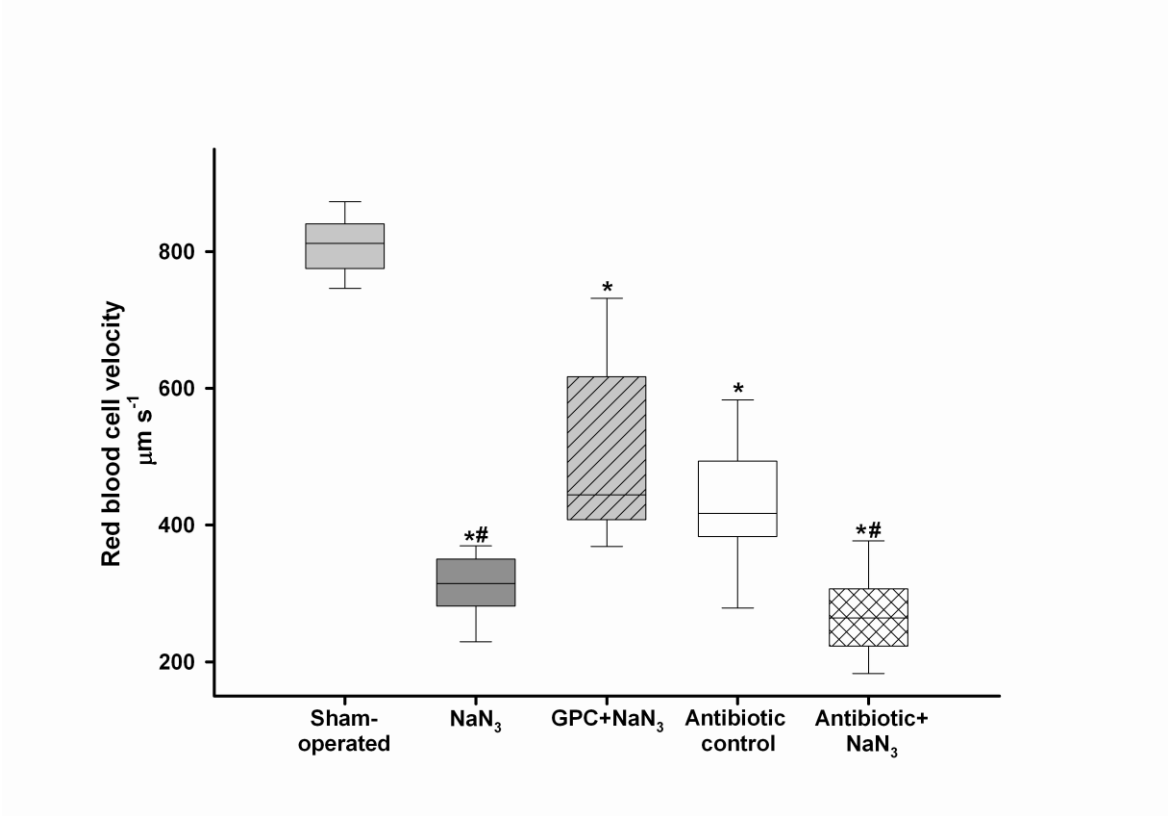

Figure 13. RBCV in the liver capillaries. The light-gray box plot relates to the sham-operated group, the dark-gray box plot to the NaN_3-treated group, the striped light-gray box plot to the GPC-treated NaN_3 group, the white box plot to the antibiotic-gavaged control group, and the checked white box plot to the antibiotic-gavaged NaN_3-treated group. Median values and 75^{th} and 25^{th} percentiles are given. $p < 0.05$ was considered statistically significant. $^{*}p < 0.05$ vs the sham-operated, or antibiotic-treated control; $^{\#}p < 0.05$ vs the GPC + NaN_3-treated group

4.3.5. Leukocyte-endothelial cell interactions after NaN_3 treatment

By day 8, the number of sticking leukocytes in the central venules was markedly enhanced in some of the NaN_3-treated animals, but the increase was not significant statistically ($p = 0.051$) due to the large interindividual differences (data not shown). The results indicated that the extent of leukocyte adhesion did not differ in the GPC + NaN_3-treated group from that in the untreated controls (data not shown).

4.3.6. In vivo morphological changes

The structure of the liver was evaluated by means of *in vivo* imaging, using confocal laser scanning endomicroscopy. The NaN_3 treatment itself did not alter the thickness of the sinusoids in the chosen areas (data not shown). The *in vivo* histology of the rats treated with NaN_3 did not reveal any tissue damage and there were no visible differences in the integrity of the hepatic portal triads between the control and treated groups (**Figure 14**).

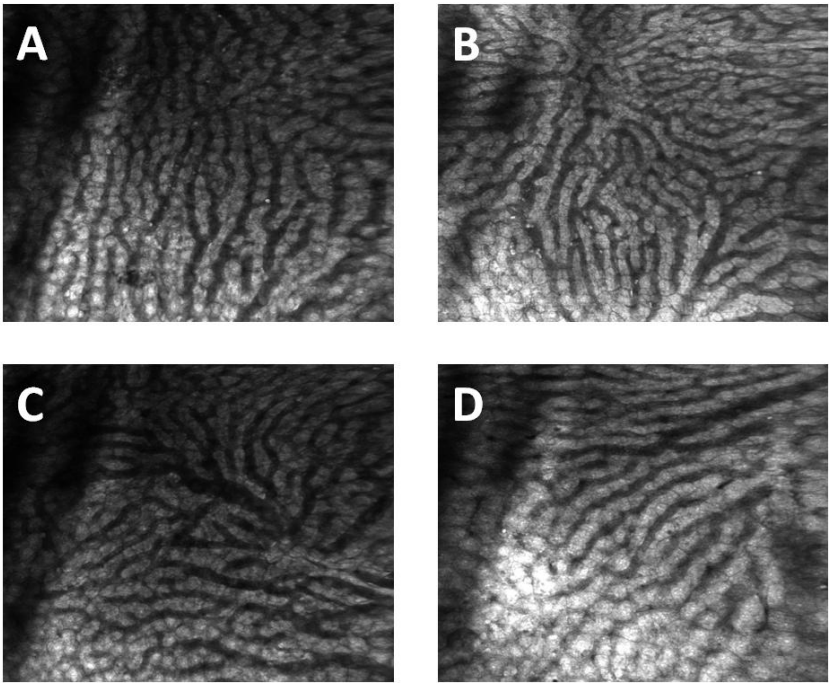

Figure 14. *In vivo* histology images of the liver lobules after acridine orange staining. A: sham-operated, B: 8 days after NaN_3 challenge, C: GPC + NaN_3 treatment, D: antibiotic + NaN_3 sample. No structural differences were detected between the groups. The thickness of the sinusoids was unchanged.

4.4. The effects of GPC on IR consequences

4.4.1. ATP level in the liver

In consequence of ischemia, the ATP level in the IR group (M: 1206.74; p25: 1093.51; p75: 1521.03) was significantly lower than that in the sham-operated group (M: 2025.03; p25: 1775.28; p75: 2232.52) at the end of the reperfusion. As compared with the IR group, there was a tendency to an elevation in the GPC + IR group (M: 1690.78; p25: 1410.30; p75: 1991.19) and a significantly higher ATP level in the IR + GPC group (M: 1977.41; p25: 1802.51; p75: 2133.95). No difference was detected between the levels in the IR + GPC and sham-operated groups **(Figure 15**).

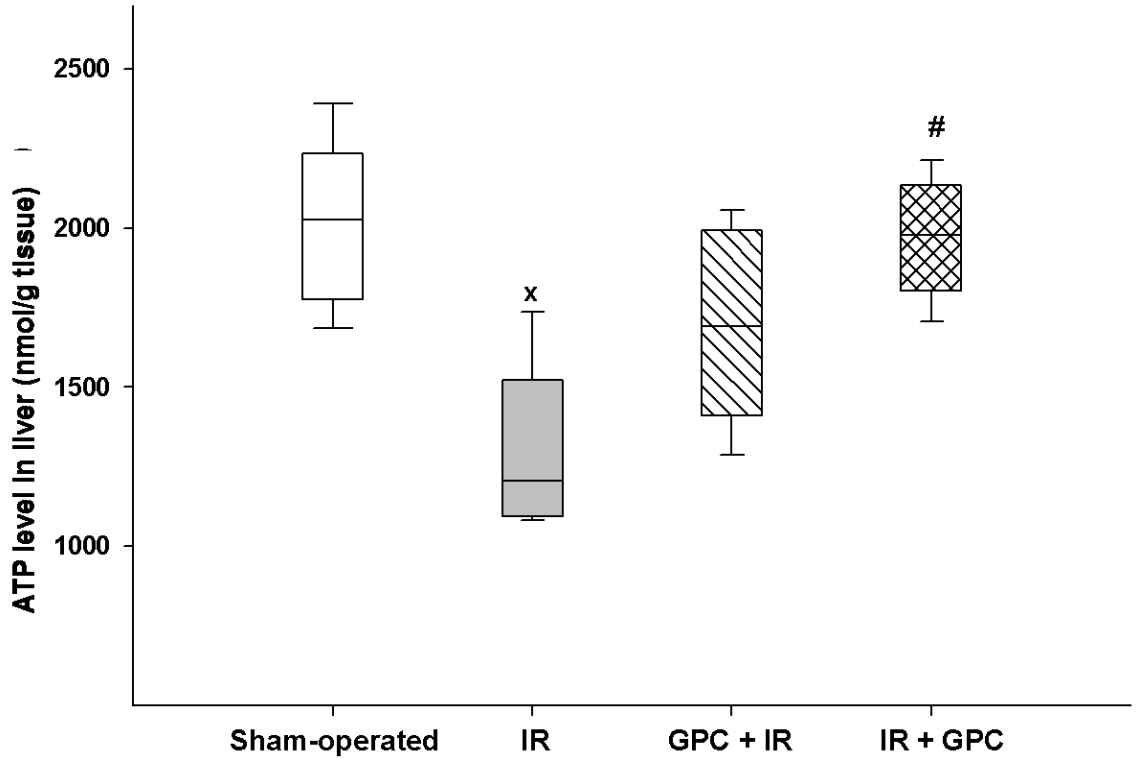

Figure 15. ATP level in liver samples. The white box blot relates to the sham-operated group, the dark-gray box plot to the IR group, the striped box plot to the GPC-pretreated group and the checked box plot to the GPC-post-treated group. Median values and 75th and 25th percentiles are given. $^{x}p < 0.05$ relative to the sham-operated control group; $^{\#}p < 0.05$ relative to the IR group.

4.4.2. XOR activity in the small intestine after IR

XOR is activated during IR and produces a considerable amount of . At the end of the experiments, we observed a significantly higher XOR activity in the IR animals (M: 78.6; p25: 67.7; p75: 80.2) than in the sham-operated ones (M: 41.8; p25: 27.3; p75: 55.9). The XOR activity was also significantly elevated in the GPC + IR group (M: 78; p25: 72; p75: 84). In contrast, the XOR activity was significantly lower in the IR + GPC group (M: 19; p25: 14; p75: 21) than in either the IR or the GPC + IR groups. The IR + GPC treatment proved highly effective against ROS-producing mechanisms (**Figure 16**).

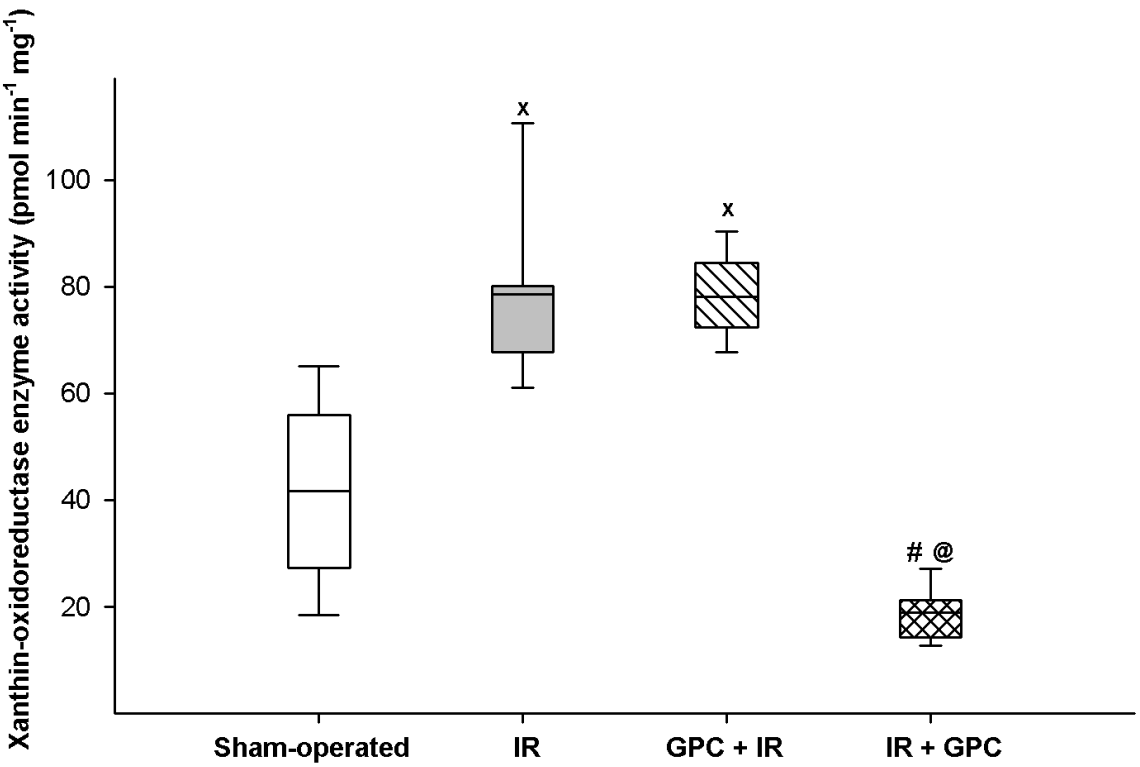

Figure 16. XOR activity in the small intestine. The white box blot relates to the sham-operated group, the dark-gray box plot to the IR group, the striped box plot to the GPC-pretreated group and the checked box plot to the GPC-post-treated group. Median values and 75^{th} and 25^{th} percentiles are given. $^{x}p < 0.05$ relative to the sham-operated control group; $^{\#}p < 0.05$ relative to the IR group; $^{@}p < 0.05$ relative to the GPC pre-treated group.

4.4.3. $O_2^{\cdot -}$: *production in the small intestine*

The ROS-producing capacity of the small intestinal biopsy samples did not change in the sham-operated animals. By 15 min of reperfusion, there was a significant enhancement in the IR group (M: 2019.4; p25: 1814.5; p75: 2349.3) relative to the baseline value and also the sham-operated group (M: 1182.2; p25: 1046.6; p75: 1340). Both GPC + IR (M: 958; p25: 856; p75: 1476) and IR + GPC treatment (M: 1228; p25: 839; p75: 1568) resulted in an appreciable reduction in the $O_2^{\cdot -}$ level as compared with the IR group. This tendency was maintained until the end of the experiments (**Figure 17**).

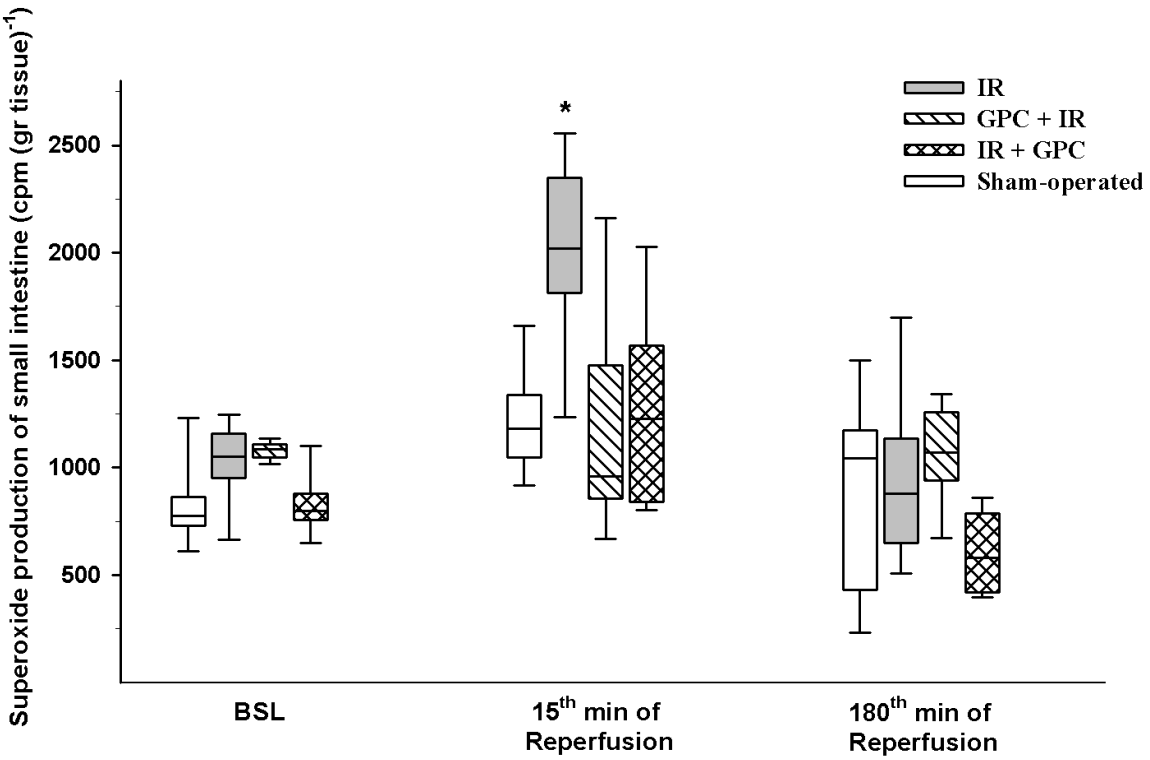

Figure 17. $O_2^{\cdot -}$ production in the small intestine. The white box blot relates to the sham-operated group, the dark-gray box plot to the IR group, the striped box plot to the GPC-pretreated group and the checked box plot to the GPC-post-treated group. Median values and 75th and 25th percentiles are given. $^{*}p < 0.05$ relative to the baseline value (within groups).

4.5. The effects of GPC on the challenge of Gamma-irradiation

4.5.1. Liver ATP levels after brain irradiation

Figure 18 reveals that brain irradiation with 40 Gy resulted in a significant reduction in hepatic ATP level as compared with the saline-treated group (M: 71.9; p25: 57.7; p75: 100.9 vs M: 120.4; p25: 117.5; p75: 126.6). In the GPC-treated group, the level of liver ATP was significantly higher and did not differ significantly from that observed in the control group (M: 119.4; p25: 113.1; p75: 123.2).

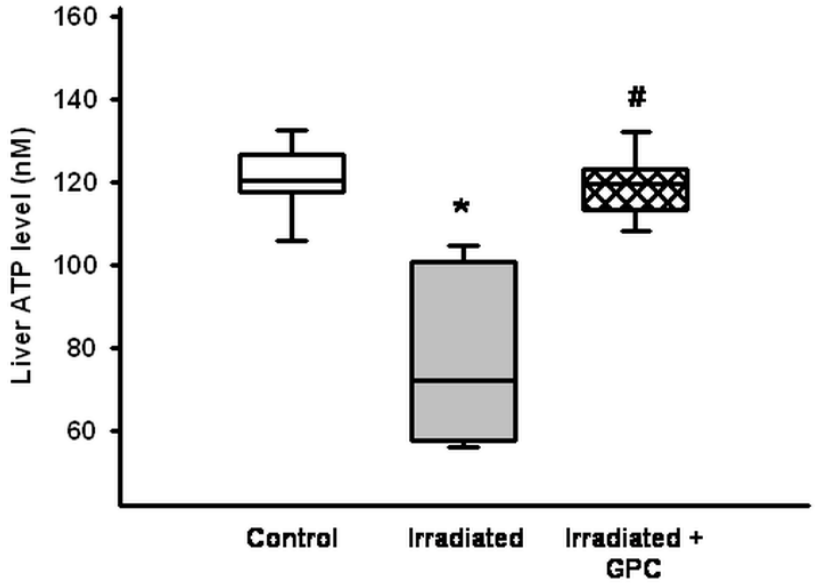

Figure 18. Liver ATP levels 3 h after 40-Gy hippocampus irradiation. The white box blot relates to the saline-treated group, the dark-gray box plot to the irradiated group and the gray box plot to the GPC-treated group. Median values and 75^{th} and 25^{th} percentiles are given. $^{*}p < 0.05$ relative to the saline-treated control group. $^{\#}p < 0.05$ relative to the irradiated group.

V. DISCUSSION

Biomarkers are useful tools through which to gain an understanding of human or animal pathophysiology and the biological response to therapy, and in this sense the significance of biotic CH_4 production is currently acquiring increased attention. Mammalian methanogenesis is closely associated with the activity of intestinal anaerobic bacteria, but previous studies have demonstrated the generation of nonbacterial CH_4 in aerobic living systems, and this phenomenon may therefore be associated with a loss in mitochondrial function (Ghyczy, 2003; Keppler, 2006; Ghyczy, 2008b; Lenhart, 2009). Nevertheless, whereas microbial methanogenesis has been reasonably well described, the details of the mechanism of aerobic CH_4 generation are basically undefined, and cellular sources are at present a subject of investigation.

5.1. Earlier studies on nonmicrobial methanogenesis

Mammalian methanogenesis is considered to be an exclusive indicator of GI carbohydrate fermentation by the anaerobic flora. This commonly held notion, however, was challenged when *in vitro* and *in vivo* studies and other investigations revealed the possibility of nonmicrobial CH_4 formation in mitochondria, eukaryote cells, plants and animals. It was shown in 2003, that hypoxia can lead to the generation of measurable amounts of nonbacterial CH_4 in isolated rat liver mitochondria (Ghyczy, 2003). When the possible causes were explored, high amounts of CH_4 were reproducibly generated after the addition of ascorbic acid and H_2O_2, and the formation was linearly related to the quantity of mitochondria incubated, the amount of H_2O_2 added and the pH of the reaction mixture. Catalase, which decomposes H_2O_2, abolished the increase in CH_4 production, which indicated that mitochondrial H_2O_2 is required for the hypoxic activation of the CH_4-generating reaction. It is important that the rate of H_2O_2 formation in rat liver tissue is ~380 nmol min^{-1} g $tissue^{-1}$ (i.e. 10% of the total O_2 consumption) and catalase is absent in the mitochondrial matrix. In 2008, further studies demonstrated aerobic CH_4 emission in cultured endothelial cells under hypoxia and metabolic distress (Ghyczy, 2008a). The latter included the inhibition of glucose uptake and anaerobic glycolysis, the application of site-specific inhibitors of the METC, alone or in combination with glycolysis inhibitors, the application of an uncoupling agent, and the treatment of the cells with increasing concentrations of the hydroxyl radical-generating Udenfriend system. These studies provided evidence of stress-induced nonbacterial CH_4 production in eukaryotes. The results showed that a disturbance of the normal mitochondrial function leads to significant CH_4 generation (in the range ~2-23 nmol mg^{-1}) in the endothelial cells, depending on the type and intensity of metabolic distress, and similarly high and dose-dependent CH_4 generation was measured after the free radical attack of the Udenfriend reaction.

In 2006, direct CH_4 emission was reported from plants under aerobic conditions (Keppler, 2006). This was followed by many studies that either supported or disagreed with the initial findings (Dueck, 2008; McLeod, 2008; Bruggeman, 2009; Messenger, 2009), but several stable isotope studies have now confirmed the possibility of plant-derived nonbacterial CH_4 formation (Whiskermann, 2011; Bruhn, 2012).

In parallel with these studies, significant CH_4 release was demonstrated in whole animals under mitochondrial stress (Boros, 1999; Ghyczy, 2008b), where exhaled or released CH_4 changes were detected *in vivo*. In the first pilot study, breath CH_4 was measured in the

exhaled air during closed-circuit anesthesia, and in a further IR group the animals were pretreated with antibiotics targeting the intestinal CH_4-generating bacterial flora. Chemically-prevented hypoxia/reoxygenation or IR initiates a complex biochemical cascade reaction in which the perturbed mitochondrial electron carrier machinery leads to the generation of ROS and other radicals. Following the hypoxia-reoxygenation cycle, the influx of activated PMN leukocytes is accompanied by further ROS formation in the reperfused tissues. These antigen-independent responses interact with and amplify each other, finally leading to impaired microhemodynamics, functional and structural cell damage, and remote or systemic inflammatory complications. Indeed, experimental studies are usually conducted to analyze ROS-induced reactions and the *in vivo* effectiveness of anti-inflammatory or antioxidant therapies on the tissue integrity and function. Reperfusion was found to be associated with a significant increase in breath CH_4 and the concentration was similar to that observed in nontreated IR animals (Boros, 1999). In another large animal model of intestinal vascular occlusion and reperfusion, the results provided further evidence that temporary ischemia leads to significant CH_4 liberation in the exhaled air during the early phase of reoxygenation (Ghyczy, 2002). Additional data demonstrated that exogenous CH_4 confers protection against the development of inflammation following an IR insult (Boros, 2012). This effect may be at least partly mediated by the immune system, as the same study demonstrated that exogenous CH_4 inhibits leukocyte activation *in vitro* (Boros, 2012).

5.2. CH_4 measurements

5.2.1. PAS-based CH_4 measurements

The tracking of the changes in CH_4 generation with GC or other, traditional gas detection methods is quite laborious and imprecise. GC is one of the most widely-used analytical methods for the determination of small amounts of organic substances such as CH_4 in gas samples. The presented PAS-based instrument proved its applicability in three studies in which it could successfully substitute a gas chromatograph. It allows *in situ* and dynamic measurements, and the gas-sampling procedure does not demand the use of disposable bags or syringes and operates without chemicals. The possible inaccuracies associated with adsorption-desorption processes were minimized by using inert materials for the setup. The use of the instrument does not require technical skill, and the utilization of commercially available, near-infrared diode lasers keeps the costs relatively low.

In our studies, the detected CH_4 changes were reproducible; the instrument is highly specific for CH_4 and has a wide dynamic range, from levels of a few ppm to several thousands

of ppm. In view of the long-term stability, control calibration is recommended only once a year. The range of application can easily be expanded by the addition of another light source to the system. PAS-based sensors have proved to be appropriate for multicomponent analyses of widely varying gas compositions (Besson, 2004; Scotoni, 2006; Hanyecz, 2010; Hirschmann, 2010; Kosterev, 2010), indicating the potential for more complex gas analysis. The sampling chamber and the flow rate of the gas samples can be optimized for different experiments. Furthermore, the instrumentation can be used in acute or chronic experiments without exposing the animals to surgery, anesthesia or other trauma during the measurements.

5.2.2. Whole-body CH_4 measurement in unrestrained rats

In our study, the whole-body CH_4 generation of living, healthy rats was determined for the first time. In order to investigate the possible changes in CH_4 generation within a one-day interval, we included 4 healthy rats into the study and the CH_4 levels were recorded every second hour on two consecutive days. Data on the CH_4 metabolism of rats are lacking and no studies have been published where rats were considered to be CH_4 producers. We therefore analyzed the CH_4-producing capacity of these animals without exposure to any stress, before and after feeding, and also in their active and passive periods. We did not detect significant CH_4 emission (between 1.007 dppm/1000 dm^2 and 1.394 dppm/1000 dm^2) at baseline and did not find any changes in the whole-body CH_4 production regardless of the hour of the day. Thus, we regarded the result as proof of the lack of methanogenic flora in our laboratory rat strain.

5.2.3. Human CH_4 measurements

Even though the determination of the whole-body CH_4 release of anesthetized or unrestrained smaller animals provides more comprehensive data in a living system, the breath test is the method of choice with which to monitor human CH_4 production (de Lacy Costello, 2013). In clinical practice, breath gas analysis has been widely used for the screening of patients with irritable bowel disease, where the observation of CH_4 concentration changes in relationship with other gaseous compounds can promote the diagnosis (Peled, 1987; Bratten, 2007). The CH_4 concentration in the breath is usually greater than 1 ppm in only 30-60% of humans (de Lacy Costello, 2013). Regardless of sex and age, we found 21% producers, with a mean CH_4 concentration of 15.4 ppm. This proportion is broadly in line with recent findings based on GC measurements, where the average breath CH_4 concentration in adult CH_4 producers was 16.6 ppm (Levitt, 2006). Large differences in breath gas analysis data are presumably due to the variations in the personal background, but possibly also to inaccuracies

of sampling and analysis techniques. Indeed, in another, comprehensive GC study, the prevalence of CH_4 producers in different ethnic groups was scattered from 24% to 58% (Pitt, 1980). Given this background, the PAS system was tested for breath analysis, in order to collect representative data for a larger, comparative human survey, and the method proved to be suitable for the analysis of single breath samples too.

5.3. Mitochondrial distress-associated CH_4 generation

After the development of an appropriately specific and sensitive PAS-based detection system for CH_4, we investigated the functional role of mitochondrial electron transport in the biogenesis. We set out to determine the *in vivo* CH_4 production profile after the induction of inflammation and/or mitochondrial distress in rodents. Here we assumed that CH_4 excretion in the breath reflects intestinal bacterial fermentation plus an unknown and variable amount of nonbacterial generation induced from target cells. We demonstrated that CH_4 generation is significantly increased in the groups exposed to a chronic NaN_3 challenge. The phenomenon proved to be independent from the methanogenic flora, since CH_4 emission was also elevated in the antibiotic-treated group. As endotoxemia and the specific inhibition of the mitochondrial complex IV lead to an increased CH_4 output, we assume that mitochondrial distress and the following inflammatory reaction might be the common denominator of CH_4 biogenesis.

5.3.1. The effect of LPS-induced endotoxemia on CH_4 generation

LPS and acute endotoxemia activate cellular toll-like receptors and induce a generalized inflammatory reaction with ROS production from multiple sources. When CH_4 exhaled from the airways together with the amounts discharged through the skin and body orifices were quantified by means of a whole-body CH_4 detection setup, acute endotoxemia was accompanied by an increasing emanation of endogenous CH_4 throughout the experiments. The use of rifaximin, an antibiotic targeting the methanogenic bacterial flora, caused a decrease in CH_4 output, but the production significantly exceeded the control and background values. These findings led us to assume that nonbacterial CH_4 was added to the bacterial production, and this addition could occur at such a rate that it was impossible to detect it by the conventional techniques utilized to look for it to date.

5.3.2. The effect of chronic NaN_3 treatment on CH_4 generation

In the next series of studies, we set out to determine the *in vivo* CH_4 production profile of the animals after the induction of mitochondrial distress by chronic inhibition of mitochondrial cytochrome c oxidase. Through determination of the amounts of CH_4 released from the

animals at the different times, our study demonstrated that a mitochondrial dysfunction was accompanied by an increasing emanation of endogenous CH_4. Changes in leukocyte reactions were chosen as endpoints via which to characterize the pro-inflammatory potential of the NaN_3 protocol. These phenomena coexist in the inflammatory milieu, and various data suggest a multiple connection between them in oxidoreductive stress-induced inflammation and evolving tissue injury. Through determination of the amounts of CH_4 released from the animals at the different times, our study demonstrated that chronic NaN_3 administration was accompanied by an increasing emanation of endogenous CH_4 throughout the entire duration of the experiments.

It is well established that NaN_3 administration can lead to the production of mitochondrial ROS in different experimental setups (Weinstock, 2004; Prigol, 2008; Ji, 2011). In our study the NaN_3-induced overall mitochondrial dysfunction was evidenced by hepatic ATP depletion, and a systemic inflammatory reaction. Direct *in vivo* evidence was also obtained for the deranged liver microcirculation, while the higher XOR and MPO activities indirectly demonstrated the impact of cytochrome c oxidase inhibition on ROS generation in several tissues. It should be noted that, despite the considerable leukocyte accumulation, quantitative tissue damage did not occur and mortality was not observed in this model. Confocal laser scanning endomicroscopy based on tissue fluorescence makes use of local contrast agents to produce very high-resolution images relative to conventional histopathology, and no signs of severe tissue loss or structural damage were detected with this technique. It is also important to mention that significant CH_4 formation was detected, irrespective of the concomitant antibiotic treatment targeting the potentially CH_4-producer GI bacterial flora. Thus, the overall evidence from these findings suggests that the CH_4-generating capacity of NaN_3 administration is independent of the methanogenic archeae, but may be associated with the NaN_3-induced generation of potentially damaging ROS.

5.4. The possible mechanism of nonbacterial CH_4 generation. The oxidoreductive stress

In the mitochondria, substrate oxidation by the METC creates a proton gradient across the inner membrane and fuels ATP synthesis by F_0F_1-ATP synthase. The transport through which the electrons shuttle must be in a steady state as regards the input of electrons and the availability of the electron acceptor O_2. A continuing lack of O_2 will cause an abnormally elevated mitochondrial $NADH/NAD^+$ ratio and the collapse of ionic homeostasis, leading to dissipation of the transmembrane potential. However, mitochondria are not only targets, but

also sources of oxidoreductive stress, and mitochondrial ROS generation is implicated in a wide variety of diseases, acute or chronic stress and IR injuries (Boland, 2013; Dikalov, 2013; Mukherjee, 2013; Ngo, 2013; Wang, 2013; Huang, 2014). A number of conditions lead to impairment of the redox homeostasis, thereby inducing the formation of ROS by transferring the excess electrons to O_2 outside the transport chain, to a site where PC or free choline is present. It must be emphasized that choline may be liberated from membrane-bound PC through the redox-sensitive activation of phospholipase D, which hydrolyzes PC to phosphatidic acid and choline, and has been implicated as a signal-activated key enzyme in a wide range of physiological responses (Tappia, 2006). In conclusion, a steady state of reducing power or redox balance may be as important for the normal functioning of aerobic cells as is a constant pH. Conversely, a redox imbalance may be as common and important a feature of abnormal clinical states as is an acid-base imbalance. Attention has focused in the past on "oxidative stress". Oxidative stress has long been assumed to be the main cause of ROS activity and its damaging consequences in biological systems. The reverse imbalance, "reductive stress", is far more common and potentially life-threatening. The underlying cause of the pathological conditions which are misleadingly referred to as oxidative stress today is reductive stress or an elevated/displaced reducing equivalent. This can be normalized only by electron acceptors, where mitochondrial damage is particularly involved. The defense mechanism which may operate against such reductive stress in biological systems may be the capture of electrons by electrophilic methyl groups (EMGs) and the consequent irreversible evolution of CH_4.

The mechanisms in the background might be quite complex, ranging from inflammatory signal activation through some DNA methylation pattern and therefore gene expression changes, but nevertheless mitochondrial dysfunction-mediated stress responses may be a common denominator. LPS activates cellular toll-like receptors and induces a generalized inflammatory reaction, with the production of ROS from multiple sources (Park, 2004). The CH_4-generating capacity of NaN_3 administration may also be associated with the generation of ROS in the same way (Smith, 1997; Duranteau, 1998) and it has been hypothesized that the EMGs of biomolecules such as choline or methionine might be the carbon precursors (Ghyczy, 2003; Bruggeman, 2009) and a potential source of CH_4 generation in this scenario. The main effect of NaN_3 is the direct inhibition of the activity of the METC through irreversible binding to the heme cofactor of cytochrome c oxidase (Bennett, 1996); thus, it can be considered a specific tool with which to study mitochondrial oxidoreductive

stress. Moreover, it has been demonstrated in human platelets that NaN_3 is capable of activating the cyclic guanosine monophosphate/cyclic guanosine phosphate-dependent protein kinase/vasodilatator-stimulated phosphoprotein pathway, which is in correlation with endogenous NO synthesis (Russo, 2008). VanUffelen and co-workers reported in 1998, that NaN_3 can be oxidized in the presence of H_2O_2 and catalase, which might also lead to NO formation and control cell respiration (Carr, 1990; Ignarro, 1999). NO is able to interact directly with cytochrome c oxidase in a very fast way, thereby competes with O_2 until free NO is available (Sarti, 2003). Moreover, NO induces an impairment of ATP synthesis, and eventually opening of the membrane transition pore, with apoptosis and cell death (Moncada, 2002). The use of rifaximin, a previously used antibiotic, caused a decrease in CH_4 release after clinical application, but the production still significantly exceeded the control and background values, probably due to sensitization. These findings led us to assume that nonbacterial CH_4 production occurred besides the bacterial production. The initial *in vitro* studies led to the proposal that EMGs bound to positively-charged nitrogen moieties (as in choline molecules) may potentially act as electron acceptors, and that these reactions may entail the generation of CH_4 (Ghyczy, 2001; 2003). A continuous lack of the electron acceptor O_2 will maintain an elevated mitochondrial NADH/NAD^+ ratio, causing reductive stress and the formation of a nucleophilic hydride ion, which may be transferred to the EMG. Thus, priming during hypoxia occurs as a progressive process involving depressed electron transport in the setting of PC breakdown, the loss of cytochrome c and antioxidants, and the triggering of CH_4 release during reoxygenation or reperfusion. It is possible, therefore, that the formation and constant building-up of ROS in the mitochondria are part of a reaction, which furnishes CH_4.

To summarize the previous findings, METC inhibition causes ROS production and serious membrane loss due to ROS-induced lipid peroxidation. Peroxidation is an immediate chain reaction; in a short time it causes a fundamental breakdown of biomembranes, leading to decompartmentalization, loss of integrity and cell death. As a consequence, membrane sparing and recovery are particularly important tasks in oxidoreductive environments. In order to avoid the potentially fatal outcome of an increased oxidoreductive potential, molecular participants of a living system should be quickly brought into use to save or regenerate membranes, which are responsible not only for separation, but also for the maintenance of a steady state via channels, pores and membrane proteins. Theoretically, all of the molecules which are potential components of phospholipid bilayers might be re-utilized. During such

processes, compounds rich in ethyl and methyl groups can be reduced by electron acceptance. This yields molecules used to seal or build up membranes, together with fully reduced CH_4 (Ghyczy, 2001). Thus, we may assume that CH_4 is the end-product of a protective mechanism linked to a membrane defense or regeneration process during ROS-induced damage.

5.5. The effects of GPC on CH_4 formation and inflammatory consequences of oxidoreductive stress

We demonstrated the ability of GPC to effectively silence several inflammatory consequences linked to a reaction that might involve cellular or mitochondrial ROS generation. GPC is a centrally-acting cholinergic precursor which increases the tolerance to ischemic tissue damage (Onishchenko, 2008). Clinically, it is effective in cerebrovascular and neurodegenerative diseases (Parnetti, 2001; De Jesus Moreno Moreno, 2003), including ischemic stroke (Barbagallo Sangiorgi, 1994). More importantly, GPC can act as a choline source in various tissues (Bauernschmitt, 1993; Lee, 1993; Amenta, 1994).

5.5.1. The effects of GPC on the stress consequences of chemical hypoxia

When this water-soluble, deacylated PC analog was administered in chemical hypoxia, the microcirculatory dysfunction, the increase in the activity of the ROS-producer XOR and the accumulation of leukocytes were all moderated. Moreover, the extent of CH_4 generation in NaN_3-treated animals was reduced concomitantly. This outcome reinforces the above-mentioned membrane regeneration-accompanied CH_4 release conception, since the level of CH_4 formation was lower and the inflammatory reaction secondary to chemical hypoxia was diminished in the GPC-treated animals. It is also substantial that the significant ATP depletion was markedly improved by GPC administration in all the mitochondrial dysfunction models we investigated.

GPC is the most bioavailable source of choline (Bauernschmitt, 2003), which can be directly or indirectly involved in the reconstruction of injured phospholipid bilayers. Accordingly, in the presence of higher intracellular GPC concentrations, the degradation of endogenous, membrane-forming compounds that could eventually have resulted in the emission of CH_4 was reduced. It should be added that exogenous PC also exerted an anti-inflammatory influence in the GI tract and significantly decreased the exhaled CH_4 concentration in a canine model of intestinal IR and our rat model of chemical hypoxia (Ghyczy, 2008; Kovács, 2012).

However, it is not clear whether GPC selectively influences the CH_4 metabolism because it can modulate other processes (e.g. blood flow-dependent or other biochemical

pathways) involved in IR-mediated injury. Indeed, it has been reported (Cao, 1987) that the PC metabolism in the rat heart is regulated by vitamin E, which has been shown to be less effective against oxidoreductive stress if no added PC is present (Shea, 2002). This suggests that GPC can also cooperate with vitamin E-mediated antioxidant protection by stabilizing membranes.

5.5.2. The effects of GPC on the inflammatory consequences of intestinal IR

As regards the IR study, the ATP level of the liver was significantly decreased in the untreated animals by the end of the reperfusion, and a tendency for ATP production to increase was seen in the GPC-treated animals. These findings may be linked to the membrane-conserving effect of GPC under oxidoreductive stress conditions. During reoxygenation, the components of the METC in the inner membrane are the main targets of ROS and reactive nitrogen species (RNS) (Raffaelo, 2011). If prolonged, such stress attacks lead to the otherwise reversible damage of the METC becoming irreversible, and functionless membranes and embedded proteins cannot synthesize ATP. Nevertheless, the METC- or membrane-protective action of GPC, including the inhibition of mitochondrial ROS or RNS formation, demands further, in-depth investigations.

5.5.3. The effects of GPC on the ATP content after gamma-irradiation

Irradiation-caused ROS accumulation and membrane damage are highly involved in the adverse effect of this kind of therapy (Pandey, 2004). The structural and functional properties of membrane lipids regulate crucial signaling processes controling the cellular fate. Radiation leads to a huge accumulation of ROS and substantial evidence has come to pass to demonstrate the active regulation of cellular radiosensitivity by the oxidative signals generated on cell membranes (Mishra, 2004). Damage to biomolecules such as proteins and lipids of membranes by radiation-induced ROS has been shown to initiate a cascade of biochemical reactions and signaling events, resulting in a loss of cellular functions and eventually cell death (Pandey, 1999, 2003; Stark, 1991).

The hippocampus is particularly sensitive to oxidoreductive stress, and ionizing irradiation with 40 Gy caused an impairment of the METC, since we observed a significant decrease in liver ATP production. Further functional, distant or long-term consequences of this phenomenon have not been fully clarified, but irradiation-induced ATP depletion was significantly reduced by GPC, which suggests that GPC supplementation can modulate the inflammatory consequences of irradiation-related liver injury. It has also been shown that GPC accumulates in the organs of excretion and the liver contains the highest metabolite

concentration (Abbiati, 1993). Under physiological conditions, GPC is involved in the preservation of the structural integrity of cellular membranes through the stimulation of PC synthesis via the Kennedy pathway (Gibbellini, 2010). Additionally, its role in the maintenance of phospholipid homeostasis has been demonstrated indirectly, since the liver concentrations of GPC are diminished after hemorrhagic shock (Scribner, 2010). The exact mechanism of GPC interference with hepatic ATP depletion is still unknown, but a possible explanation might be the membrane regenerative capacity, in which the METC function is maintained.

VI. SUMMARY OF THE NEW FINDINGS

1. We have developed and used a new diagnostic procedure based on PAS for the real-time detection of CH_4 generation. With this technique, the daily CH_4 output can be determined and different stress-caused changes or treatment effects can be evaluated accurately and reproducibly.

2. The PAS-based spectroscopic method proved to be appropriate for reproducible and reliable breath CH_4 analysis in humans. The exhaled CH_4 concentration of a heterogeneous human population was monitored and the ratio of CH_4 producers was determined. There was no difference in the CH_4-producer ratio from the aspect of the sex, but significantly more CH_4 producers were found in the adult population as compared with those aged under 21 years.

3. The whole-body CH_4 emission profile of rodents was detected for the first time. The baseline CH_4 generation of rats and mice and also the changes in the CH_4 values after exposure to various chronic challenges inducing mitochondrial dysfunctions were determined.

4. The CH_4 level was significantly increased under oxidoreductive stress conditions, independently of the methanogenic bacterial production. This phenomenon might be an alarm signal linked to the earlier phase of oxidoreductive stress states.

5. The administration of GPC terminated stress-associated CH_4 generation in rodents, and alleviated the inflammatory consequences of acute oxidoreductive stress. The pro-oxidant enzyme activity and $O_2^{\cdot -}$ level were reduced and the liver ATP content was maintained on GPC treatment. Accordingly, GPC supplementation may provide protection against hypoxia or irradiation-caused stress conditions and might be a promising therapeutic agent with which to influence such events.

VII. ACKNOWLEDGMENTS

First and foremost, I would like to express my gratitude to my principal supervisor, Professor Mihály Boros, whom I consider to be the best mentor in the world. Besides his patient guidance and encouragement, he could always keep me smiling and motivated.

The members of the Institute of Surgical Research have contributed immensely to my personal and professional activities. The team has been a source of friendships, good advice and collaboration. I would especially like to thank Dr. József Kaszaki, who introduced me to the real experimental work.

I would like to give my sincere thanks to Anna Szabó and Dr. Árpád Mohácsi, my two great physicist colleagues, without whom my experimental ideas would have remained pure fantasy.

This work would not have been possible without the help and support of my clinician and researcher colleagues here in Szeged and also abroad. I have been able to learn and develop considerably through this and I would never have achieved my goals without them.

This journey from the university years until becoming a researcher was made enjoyable in large part due to the many friends and groups that have become a part of my life. I owe my special thanks to Dóra Haluszka, Gábor Kisvári, Ádám Horváth and Gábor Tax. With them, I shared not only the school desk, but also my flat and my life.

Likewise, I wish to thank Petra Sántha, Eszter Fodor, Viktória Nagy, Szilárd Zerinváry and Dénes Garab for the support and friendship they have lent me from the very beginning.

I would like especially to thank my best-ever colleague and great friend, Tünde Tőkés, without whom I could not got through these years. Special thanks to my trainee, Gábor Bartha. It has been a real pleasure to be his first supervisor and friend.

Last, but not least, I would like to acknowledge the part played by my family for their continuous belief and support and in particular my twin brother, the great scientist Csaba Tuboly, and my better-half, Dr Szabolcs Lehoczki-Krsjak.

This thesis was supported by TÁMOP-4.2.2/B-10/1-2010-0012, TÁMOP-4.2.4.A/ 2-11/1-2012-0001 ‘National Excellence Program’

VIII. LIST OF REFERENCES

1. Abbiati G, Fossati T, Lachmann G, Bergamaschi M and Castiglioni C: Absorption, tissue distribution and excretion of radiolabelled compounds in rats after administration of [14C]-L-alpha-glycerylphosphorylcholine. *Eur J Drug Metab Pharmacokinet.* 1993; 18:173.
2. Amenta F, Liu A, Zeng YC and Zaccheo D: Muscarinic cholinergic receptors in the hippocampus of aged rats: influence of choline alphoscerate treatment. *Mech Ageing Dev.* 1994; 76:49-64.
3. Attaluri A, Jackson M, Valestin J and Rao SS: Methanogenic flora is associated with altered colonic transit but not stool characteristics in constipation without IBS. *Am J Gastroenterol.* 2010;105:1407-11.
4. Barbagallo Sangiorgi G, Barbagallo M, Giordano M, Meli M and Panzarasa R: alpha-Glycerophosphocholine in the mental recovery of cerebral ischemic attacks. An Italian multicenter clinical trial. *Ann NY Acad Sci.* 1994; 717:253-269.
5. Bauernschmitt HG and Kinne RK: Metabolism of the 'organic osmolyte' glycerophosphorylcholine in isolated rat inner medullary collecting duct cells. I. Pathways for synthesis and degradation. *Biochim Biophys Acta.* 1993; 1148:331-41.
6. Bennett MC, Mlady GW, Kwon YH and Rose GM: Chronic in vivo sodium azide infusion induces selective and stable inhibition of cytochrome c oxidase. *J Neurochem*. 1996; 66:2606-2611.
7. Besson J P, Schilt S and Thevenaz L: Multi-gas sensing based on photoacoustic spectroscopy using tunable laser diodes. *Spectrochim. Acta.2004;* A 60:3449–56.
8. Bindoli A: Lipid peroxidation in mitochondria. *Free Rad Biol Med*. 1988; 5: 247-261.
9. Bleier L and Dröse S: Superoxide generation by complex III: from mechanistic rationales to functional consequences. *Biochim Biophys Acta*. 2013; 1827:1320-31.
10. Bochkov VN, Kadl A, Huber J, Gruber F, Binder BR and Leitinger N: Protective role of phospholipid oxidation products in endotoxin-induced tissue damage. *Nature.* 2002; 419:77-81.
11. Boland ML, Chourasia AH and Macleod KF: Mitochondrial dysfunction in cancer. *Front Oncol*. 2013; 3:292.
12. Boros M, Ghyczy M, Erces D, Varga G, Tokes T, Kupai K, Torday C and Kaszaki J: The anti-inflammatory effects of methane. *Crit Care Med.* 2012; 40:1269-1278.

13. Boros M, Wolfárd A and Ghyczy M: In vivo evidence of reductive stress-induced methane production. *Shock.* 1999; 12:56.

14. Bozóki Z, Pogány A and Szabó G: Photoacoustic instruments for practical applications: present, potentials, and future challenges *Appl. Spectrosc. Rev.* 2011; 46:1–37.

15. Bratten J R and Jones M P: Small intestinal motility. *Curr. Opin. Gastroenterol.* 2007; 23:127–33.

16. Bruggemann N, Meier R, Steigner D, Zimmer I, Louis S and Schnitzler JP: Nonmicrobial aerobic methane emission from poplar shoot cultures under low-light conditions. *New Phytol.* 2009; 182:912-918.

17. Bruhn D , Møller IM, Mikkelsen TN and Ambus P: Terrestrial plant methane production and emission. *Physiol Plant*. 2012; 144:201-9.

18. Cao Y, O K, Choy PC and Chan A: Regulation by vitamin E of phosphatidylcholine metabolism in rat heart. *Biochem J.* 1987; 247:35-140.

19. Carr GJ and Ferguson SJ: Nitric oxide formed by nitrite reductase of Paracoccus denitrificans is sufficiently stable to inhibit cytochrome oxidase activity and is reduced by its reductase under aerobic conditions. *Biochim Biophys Acta*. 1990; 1017:57-62.

20. Ceda GP , Ceresini G, Denti L, Marzani G, Piovani E, Banchini A, Tarditi E and Valenti G: Alpha-Glycerylphosphorylcholine administration increases the GH responses to GHRH of young and elderly subjects. *Horm Metab Res*. 1992; 24:119-21.

21. Cohen BH: Pharmacologic effects on mitochondrial function. *Dev Disabil Res Rev*. 2010; 16:189-99.

22. Corbi G, Conti V, Russomanno G, Longobardi G, Furgi G, Filippelli A and Ferrara N: Adrenergic signaling and oxidative stress: a role for sirtuins? *Front Physiol.* 2013; 4: 324.

23. Cristescu S M, Persijn S T, Lintel Hekkert S T and Harren F J M: Laser-based systems for trace gas detection in life sciences *Appl. Phys.* 2008; B 92:343–9.

24. Dawson TM and Snyder SH: Gases as biological messengers: nitric oxide and carbon monoxide in the brain. *J Neurosci*. 1994; 14:5147-5159.

25. De Jesus Moreno Moreno M: Cognitive improvement in mild to moderate Alzheimer's dementia after treatment with the acetylcholine precursor choline alfoscerate: A multicenter, double-blind, randomized, placebo-controlled trial. *Clin Therapeutics.* 2003; 25:178–193.

26. de Lacy Costello BPJ, Ledochowski M and Ratcliffe N M: The importance of methane breath testing: a review *J. Breath Res.* 2006; 7:024001.

27. Denman SE, Tomkins NW and McSweeney CS: Quantitation and diversity analysis of ruminal methanogenic populations in response to the antimethanogenic compound bromochloromethane. *FEMS Microbiol Ecol*. 2007; 62:313-322.

28. Dikalov SI and Ungvari Z: Role of mitochondrial oxidative stress in hypertension. *Am J Physiol Heart Circ Physiol*. 2013; 305: H1417-1427.

29. Drago F , Mauceri F, Nardo L, Valerio C, Lauria N, Rampello L and Guidi G: Behavioral effects of L-alpha-glycerylphosphorylcholine: influence on cognitive mechanisms in the rat. *Pharmacol Biochem Behav.* 1992; 41:445-8.

30. Droge W, Kinscherf R, Hildebrandt W and Schmitt T: The deficit in low molecular weight thiols as a target for antiageing therapy. *Curr Drug Targets.* 2006; **7**:1505-1512.

31. Dröse S and Brandt U: Molecular mechanisms of superoxide production by the mitochondrial respiratory chain. *Adv Exp Med Biol*. 2012; 748:145-69.

32. Dueck T and van der Werf A: Are plants precursors for methane? *New Phytol*. 2008; 178:693-5.

33. Duranteau J, Chandel N S, Kulisz A, Shao Z and Schumacker P T: Intracellular signaling by reactive oxygen species during hypoxia in cardiomyocytes *J. Biol. Chem.* 1998; 273:11619-24.

34. Erős G, Ibrahim S, Siebert N, Boros M and Vollmar B: Oral phosphatidylcholine pretreatment alleviates the signs of experimental rheumatoid arthritis. *Arthritis Res Ther*. 2009; 11:R43.

35. Ferdinandy P, Danial H, Ambrus I, Rothery RA, Schulz R: Peroxynitrite is a major contributor to cytokine-induced myocardial contractile failure. *Circ Res*. 2000; 87:241-7.

36. Finegold SM, Molitoris D and Väisänen ML: Study of the in vitro activities of rifaximin and comparator agents against 536 anaerobic intestinal bacteria from the perspective of potential utility in pathology involving bowel flora. *Antimicrob Agents Chemother 2009;* 53:281-286.

37. Finsterer J and Segall L: Drugs interfering with mitochondrial disorders. *Drug Chem Toxicol*. 2010; 33:138-51.

38. Flourié B, Etanchaud F, Florent C, Pellier P, Bouhnik Y and Rambaud JC: Comparative study of hydrogen and methane production in the human colon using caecal and faecal homogenates. *Gut*. 1990; 31:684-5.

39. Friedrich MW: Methyl-Coenzyme M reductase genes: Unique functional markers for methanogenic and anaerobic methane-oxidizing Archaea. *Methods Enzymol*. 2005; 397:428–442.

40. Gadhia MM, Cutter GR, Abman SH and Kinsella JP: Effects of early inhaled nitric oxide therapy and Vitamin A supplementation on the risk for bronchopulmonary dysplasia in premature newborns with respiratory failure. *J Pediatr*. 2014; 164:744-8.

41. Gera L, Varga R, Török L, Kaszaki J, Szabó A, Nagy K and Boros M: Beneficial effects of phosphatidylcholine during hindlimb reperfusion. *J Surg Res*. 2007; 139:45-50.

42. Ghyczy M and Boros M: Electrophilic methyl groups present in the diet ameliorate pathological states induced by reductive and oxidative stress: a hypothesis. *Br J Nutr*. 2001; 85:409-414.

43. Ghyczy M, Czobel M and Boros M: Oral phosphatidylcholine pretreatment decreases ischemia-reperfusion-induced methane generation and the inflammatory response in the small intestine. *Shock*. 2008b; 30:596-602.

44. Ghyczy M, Torday C and Boros M: Simultaneous generation of methane, carbon dioxide, and carbon monoxide from choline and ascorbic acid: a defensive mechanism against reductive stress? *FASEB J*. 2003; 17:1124-1126.

45. Ghyczy M, Torday C, Kaszaki J, Szabo A, Czóbel M and Boros M: Hypoxia-induced generation of methane in mitochondria and eukaryotic cells: an alternative approach to methanogenesis. *Cell Physiol Biochem*. 2008a; 21: 251-258.

46. Gibellini F and Smith TK: The Kennedy pathway--De novo synthesis of phosphatidylethanolamine and phosphatidylcholine. *IUBMB Life*. 2010; 62:414.

47. Gutteridge JM: Does redox regulation of cell function explain why antioxidants perform so poorly as therapeutic agents? *Redox Rep*. 1999; 4:129-131.

48. Halestrap AP, Clarke SJ and Javadov SA: Mitochondrial permeability transition pore opening during myocardial reperfusion-a target for cardioprotection. *Cardiovasc Res*. 2004; 61: 372 – 385.

49. Hanyecz V, Mohácsi Á, Pogány A, Varga A, Bozóki Z, Kovács I and Szabó G: Multi-component photoacoustic gas analyzer for industrial applications *Vib. Spectrosc*. 2010; 52:63–8.

50. Hartmann P, Szabó A, Erős G, Gurabi D, Horváth G, Németh I, Ghyczy M and Boros M: Anti-inflammatory effects of phosphatidylcholine in neutrophil leukocyte-dependent acute arthritis in rats. *Eur J Pharmacol*. 2009; 622:58-64.

51. Hirschmann C B, Uotila J, Ojala S, Tenhunen J and Keiski R L: Fourier transform infrared photoacoustic multicomponent gas spectroscopy with optical cantilever detection *Appl. Spectrosc*. 2010; 64:293–7.

52. Huang SH, Hsu MH, Hsu SC, Yang JS, Huang WW, Huang AC, Hsiao YP, Yu CC and Chung JG: Phenethyl isothiocyanate triggers apoptosis in human malignant melanoma A375.S2 cells through reactive oxygen species and the mitochondria-dependent pathways. *Hum Exp Toxicol.* 2014; 33: 270-283.

53. Ignarro LJ, Cirino G, Casini A and Napoli C: Nitric oxide as a signaling molecule in the vascular system: an overview. *J Cardiovasc Pharmacol*. 1999; 34:879-86.

54. Ishii T, Miyazawa M, Onouchi H, Yasuda K, Hartman PS and Ishii N: Model animals for the study of oxidative stress from complex II. *Biochim Biophys Acta*. 2013; 1827:588-97.

55. Jahjah M , Ren W, Stefański P, Lewicki R, Zhang J, Jiang W, Tarka J and Tittel FK: A compact QCL based methane and nitrous oxide sensor for environmental and medical applications. *Analyst*. 2014; 139:2065-9.

56. Ji D, Kamalden TA, del Olmo-Aguado S and Osborne NN: Light- and sodium azide-induced death of RGC-5 cells in culture occurs via different mechanisms. *Apoptosis.* 2011; 16:425-437.

57. Karger CP, Münter MW, Heiland S, Peschke P, Debus J and Hartmann GH: Dose-response curves and tolerance doses for late functional changes in the normal rat brain after stereotactic radiosurgery evaluated by magnetic resonance imaging: influence of end points and follow-up time. *Radiation Research*. 2002; 157:617–625.

58. Keppler F, Hamilton JT, Brass M and Röckmann T: Methane emissions from terrestrial plants under aerobic conditions. *Nature.* 2006; 439:187-91.

59. Keppler F, Hamilton JT, McRoberts WC, Vigano I, Brass M and Rockmann T: Methoxyl groups of plant pectin as a precursor of atmospheric methane: evidence from deuterium labelling studies. *New Phytol.* 2008; 178:808-814.

60. Kidd PM: Integrated brain restoration after ischemic stroke--medical management, risk factors, nutrients, and other interventions for managing inflammation and enhancing brain plasticity. *Altern Med Rev*. 2009; 14:14-35.

61. Knyihár-Csillik E, Okuno E and Vécsei L: Effects of in vivo sodium azide administration on the immunohistochemical localization of kynurenine aminotransferase in the rat brain. *Neuroscience.* 1999; 94:269-277.

62. Kosterev A A, Dong L, Thomazy D, Tittel F K and Overby S: QEPAS for chemical analysis of multi-component gas mixtures *Appl. Phys.* 2010; B 101:649–59.

63. Kovács T, Varga G, Erces D, Tőkés T, Tiszlavicz L, Ghyczy M, Boros and Kaszaki J: Dietary phosphatidylcholine supplementation attenuates inflammatory mucosal damage in a rat model of experimental colitis. *Shock.* 2012; 38:177-85.

64. Lamon BD, Zhang FF, Puri N, Brodsky SV, Goligorsky MS and Nasjletti A: Dual pathways of carbon monoxide-mediated vasoregulation: modulation by redox mechanisms. *Circ Res.* 2009; 105:775-783.

65. Le Marchand L, Wilkens L R, Harwood P and Cooney R V: Use of breath hydrogen and methane as markers of colonic fermentation in epidemiologic studies: circadian patterns of excretion *Environ. Health Perspect.* 1992; 98:199–202.

66. Lee HC, Fellenz-Maloney MP, Liscovitch M and Blusztajn JK: Phospholipase D-catalyzed hydrolysis of phosphatidylcholine provides the choline precursor for acetylcholine synthesis in a human neuronal cell line. *Proc Natl Acad Sci USA.* 1993; 90:10086-10090.

67. Lenhart K, Bunge M, Ratering S, Neu TR, Schüttmann I, Greule M, Kammann C, Schnell S, Müller C, Zorn H and Keppler F: Evidence for methane production by saprotrophic fungi. *Nat Commun.* 2012; 3:1046.

68. Levitt M D, Furne J K and Kuskowski M J: Stability of human methanogenic flora over 35 years and a review of insights obtained from breath methane measurements *Clin. Gastroenterol. Hepatol.* 2005; 4:123–9.

69. Ligor T, Ligor M, Amann A, Ager C, Bachler M, Dzien A and Buszewski B: The analysis of healthy volunteers' exhaled breath by the use of solid-phase microextraction and GC-MS *J. Breath Res. 2008;* 2:046006.

70. Liu Y , Luo HS, Liang CB, Tan W, Xia H, and Xu WJ: Effects of methane on proximal colon motility of rats and ion channel mechanisms. *Zhonghua Yi Xue Za Zhi*. 2013 93:459-63.

71. Mathur R, Amichai M, Chua KS, Mirocha J, Barlow GM and Pimentel M: Methane and hydrogen positivity on breath test is associated with greater body mass index and body fat. *J Clin Endocrinol Metab*. 2013; 98:E698-702.

72. McLeod AR, Fry SC, Loake GJ, Messenger DJ, Reay DS, Smith KA and Yun BW: Ultraviolet radiation drives methane emissions from terrestrial plant pectins. *New Phytol*. 2008; 180:124-132.

73. Messenger DJ, McLeod AR and Fry SC: The role of ultraviolet radiation, photosensitizers, reactive oxygen species and ester groups in mechanisms of methane formation from pectin. *Plant Cell Environ.* 2009; 32:1-9.

74. Mishra KP: Cell membrane oxidative damage induced by Gamma-Radiation and apoptotic sensitivity. *J Environ Pathol Toxicol Oncol.* 2004; 23:1.

75. Mitchell L, Brook E, Lee JE, Buizert C and Sowers T: Constraints on the late holocene anthropogenic contribution to the atmospheric methane budget. *Science.* 2013; 342:964-966.

76. Moncada S and Erusalimsky JD: Does nitric oxide modulate mitochondrial energy generation and apoptosis? *Nat Rev Mol Cell Biol.* 2002*;* 3:214-220.

77. Morris BE, Herbst FA, Bastida F, Seifert J, von Bergen M, Richnow HH and Suflita JM: Microbial interactions during residual oil and n-fatty acid metabolism by a methanogenic consortium. *Environ Microbiol Rep.* 2012; 4:297-306.

78. Motterlini R and Otterbein LE: The therapeutic potential of carbon monoxide. *Nat Rev Drug Discov.* 2010; 9:728-743.

79. Mukherjee R and Chakrabarti O: Mitochondrial quality control: decommissioning power plants in neurodegenerative diseases. *Scientific World Journal.* 2013; 2013: 180759.

80. Münter MW, Karger CP, Reith W, Schneider HM, Peschke P and Debus J: Delayed vascular injury after single high-dose irradiation in the rat brain: histologic immunohistochemical, and angiographic studies. *Radiology. 1999;* 212:475-482.

81. Ngai A K Y, Persijn S T, von Basum G and Harren F J M: Automatically tunable continuous-wave optical parametric oscillator for high-resolution spectroscopy and sensitive trace-gas detection *Appl. Phys. 2006;* B 85:173–80.

82. Ngo JK, Pomatto LC and Davies KJ: Upregulation of the mitochondrial Lon Protease allows adaptation to acute oxidative stress but dysregulation is associated with chronic stress, disease, and aging. *Redox Biol.* 2013; 1: 258-264.

83. Nivala AM, Reese L, Frye M, Gentile CL and Pagliassotti MJ: Fatty acid-mediated endoplasmic reticulum stress in vivo: differential response to the infusion of soybean and lard oil in rats. *Metabolism* 2013; 62:753-60.

84. Nohl H, Breuninger V and Hegner D: Influence of mitochondrial radical formation on energy-linked respiration. *Eur J Biochem.*1978; 90:385-90.

85. Nose K, Nunome Y, Kondo T, Araki S and Tsuda T: Identification of gas emanated from human skin: methane, ethylene, and ethane *Anal. Sci.* 2005; 21:625–8.

86. Olszewska A and Szewczyk A: Mitochondria as a pharmacological target: magnum overview. *IU BMB Life.* 2013; 65:273-81.

87. Onischenko LS, Gaikova ON and Yanishevskii SN: Changes at the focus of experimental ischemic stroke treated with neuroprotective agents. *Neurosci Behav Physiol*. 2008; 38:49-54.

88. Onishchenko LS, Gaikova ON, Yanishevskii SN. Changes at the focus of experimental ischemic stroke treated with neuroprotective agents. *Neurosci Behav Physiol* 38: 49-54, 2008.

89. Pandey BN and Mishra KP: In vitro studies on radiation induced membrane oxidative damage in apoptotic death of mouse thymocytes. *Intl J Low Radiat.* 2003; 1:113-119.

90. Pandey BN and Mishra KP: Radiation induced oxidative damage modification by cholesterol in liposomal membrane. *Radiat Phys Chem*. 1999; 54:481-489.

91. Pandey BN and Mishra KP: Role of membrane oxidative damage and reactive oxygene species in radiation induced apoptotic death in mouse thymocytes. *BARC Newsletter*. 2004; 294:105-110.

92. Park H S, Jung H Y, Park E Y, Kim J, Lee W J and Bae Y S: Cutting edge: direct interaction of TLR4 with NAD(P)H oxidase 4 isozyme is essential for lipopolysaccharide-induced production of reactive oxygen species and activation of NF-κB *J. Immunol*. 2004; 173:3589–93.

93. Parnetti L, Amenta F and Gallai V: Choline alphoscerate in cognitive decline and in acute cerebrovascular disease: an analysis of published clinical data. *Mech Ageing Dev.* 2001; 122:2041-2055.

94. Peled Y, Weinberg D, Hallak A and Gilat T: Factors affecting methane production in humans *Dig. Dis. Sci.* 1987; 3 267–71.

95. Pfeiffer DR, Schmid PC, Beatrice MC and Schmid HHO: Intramitochondrial phospholipase activity and the effects of Ca^{2+} plus N-ethylmaleimide on mitochondrial function. *J. Biol. Chem*. 1979; 254: 11485–11494.

96. Pitt P, De Bruijn K M, Beeching M F, Goldberg E and Blendis L M: Studies on breath methane: the effect of ethnic origins and lactulose. *Gut* 1980*;* 21:951–4.

97. Prigol M, Wilhelm EA, Schneider CC and Nogueira CW: Protective effect of unsymmetrical dichalcogenide, a novel antioxidant agent, in vitro and an in vivo model of brain oxidative damage. *Chem Biol Interact.* 2008; 176:129-136.

98. Raffaello A and Rizzuto R: Mitochondrial longevity pathways. *Biochim Biophys Acta*. 2011; 1813:260-8.

99. Rocha AS , da Silva VT, Eon JG, de Menezes SM, Faro AC Jr and Rocha AB: Characterization by 27Al NMR, X-ray absorption spectroscopy, and density functional theory techniques of the species responsible for benzene hydrogenation in Y zeolite-supported carburized molybdenum catalysts. *J Phys Chem B*. 2006; 110:15803-11.

100. Rochette L, Cottin Y, Zeller M and Vergely C: Carbon monoxide: mechanisms of action and potential clinical implications. *Pharmacol Ther*. 2013; 137:133-152.

101. Russo I, Del Mese P, Viretto M, Doronzo G, Mattiello L, Trovati M and Anfossi G: Sodium azide, a bacteriostatic preservative contained in commercially available laboratory reagents, influences the responses of human platelets via the cGMP/PKG/VASP pathway. *Clin Biochem*. 2008; 41:343-9.

102. Ryter SW and Otterbein LE: Carbon monoxide in biology and medicine. *Bioessays*. 2004; 26:270-280.

103. Sahakian AB, Jee SR and Pimentel M.: Methane and the gastrointestinal tract. *Dig Dis Sci*. 2010; 55:2135-43.

104. Sarti P, Arese M, Bacchi A, Barone MC, Forte E, Mastronicola D, Brunori M and Giuffrè A: Nitric oxide and mitochondrial complex IV. *IUBMB Life*. 2003*;* 55: 605-611.

105. Scatena R, Bottoni P, Botta G, Martorana GE and Giardina B: The role of mitochondria in pharmacotoxicology: a reevaluation of an old, newly emerging topic. *Am J Physiol Cell Physiol*. 2007; 293:C12-21.

106. Scotoni M, Rossi, A, Bassi D, Buffa R, Iannotta S and Boschetti A: Simultaneous detection of ammonia, methane and ethylene at 1.63 μm with diode laser photoacoustic spectroscopy *Appl. Phys.* 2006*;* B 82:495–500.

107. Scribner DM, Witowski NE, Mulier KE, Lusczek ER, Wasiluk KR and Beilman GJ: Liver metabolomic changes identify biochemical pathways in hemorrhagic shock. *J Surg Res*. 2010; 164:131.

108. Shea TB, Ekinci FJ, Ortiz D, Dawn-Linsley M, Wilson TO and Nicolosi RJ: Efficacy of Vitamin E, phosphatidyl choline, and pyruvate on buffering neuronal degeneration and oxidative stress in cultured cortical neurons and in central nervous tissue of apopoliprotein E-deficient mice. *Free Radic Biol Med*. 2002; 33:276–282.

109. Shima S, Warkentin E, Thauer RK and Ermler U: Structure and function of enzymes involved in the methanogenic pathway utilizing carbon dioxide and molecular hydrogen. *J Biosci Bioeng*. 2002; 93:519-30.

110. Sigala S, Imperato A, Rizzonelli P, Casolini P, Missale C and Spano P: L-alpha-glycerylphosphorylcholine antagonizes scopolamine-induced amnesia and enhances hippocampal cholinergic transmission in the rat. *Eur J Pharmacol*. 1992; 211:351-8.

111. Singer M and Brealey D: Mitochondrial dysfunction in sepsis. *Biochem Soc Symp*. 1999; 66:149-66.

112. Smith T S and Bennett J P: Mitochondrial toxins in models of neurodegenerative diseases. I: in vivo brain hydroxyl radical production during sytemic MPTP treatment or following microdialysis infusion of methylpyridinium or azide ions *Brain Res.* 1997*;* 765:183-8.

113. Soares AC, Lederman HM, Fagundes-Neto U, de Morais MB: Breath methane associated with slow colonic transit time in children with chronic constipation. *J Clin Gastroenterol*. 2005; 39:512-5.

114. Stark G: The effect of ionizing radiation on lipid membranes. *Biochim Biophys Acta*. 1991; 1071:103-122.

115. Stremmel W, Ehehalt R, Staffer S, Stoffels S, Mohr A, Karner M and Braun A: Mucosal protection by phosphatidylcholine. *Dig Dis*. 2012; 30 Suppl 3:85-91.

116. Strocchi A, Furne J, Ellis C and Levitt MD: Methanogens outcompete sulphate reducing bacteria for H_2 in the human colon. *Gut*. 1994; 35:1098-1101.

117. Szabados T, Dul C, Majtényi K, Hargitai J, Pénzes Z and Urbanics R: A chronic Alzheimer's model evoked by mitochondrial poison sodium azide for pharmacological investigations. *Behav Brain Res.* 2004*;* 154:31-40.

118. Szabo C, Coletta C, Chao C, Modis K, Szczesny B, Papapetropoulos A and Hellmich MR: Tumor-derived hydrogen sulfide, produced by cystathionine-beta-synthase, stimulates bioenergetics, cell proliferation, and angiogenesis in colon cancer. *Proc Natl Acad Sci U S A*. 2013; 110: 12474-12479.

119. Tappia PS , Dent MR and Dhalla NS: Oxidative stress and redox regulation of phospholipase D in myocardial disease. *Free Radic Biol Med.* 2006; 41:349-61.

120. Tőkés T, Erős G, Bebes A, Hartmann P, Várszegi S, Varga G, Kaszaki J, Gulya K, Ghyczy M and Boros M: Protective effects of a phosphatidylcholine-enriched diet in

lipopolysaccharide-induced experimental neuroinflammation in the rat. *Shock.* 2011; 36:458-65.

121. Toogood PL: Mitochondrial drugs. *Curr Opin Chem Biol*. 2008; 12:457-63.

122. Treede I, Braun A, Jeliaskova P, Giese T, Füllekrug J, Griffiths G, Stremmel W and Ehehalt R: TNF-alpha-induced up-regulation of pro-inflammatory cytokines is reduced by phosphatidylcholine in intestinal epithelial cells. *BMC Gastroenterol.* 2009; 9:53.

123. VanUffelen BE, Van der Zee J, de Koster BM, VanSteveninck J and Elferink JG: Sodium azide enhances neutrophil migration and exocytosis: involvement of nitric oxide, cyclic GMP and calcium. *Life Sci.* 1998; 63:645-657.

124. Varga R, Gera L, Török L, Kaszaki J, Szabó A, Nagy K and Boros M: Effects of phosphatidylcholine therapy after hindlimb ischemia and reperfusion. *Magy Seb.* 2006; 59:429-36.

125. Volinsky R and Kinnunen PK. Oxidized phosphatidylcholines in membrane-level cellular signaling: from biophysics to physiology and molecular pathology. *FEBS J*. 2013; 280:2806-16.

126. Wallace DC: Mitochondria as chi. *Genetics.* 2008; 179:727-35.

127. Wang J, Lu S, Moenne-Loccoz P and Ortiz de Montellano PR: Interaction of nitric oxide with human heme oxygenase-1. *J Biol Chem*. 2003; 278:2341-2347.

128. Wang R: Gasotransmitters: growing pains and joys. *Trends Biochem Sci*. 2014; 39:227-32.

129. Weinstock M and Shoham S: Rat models of dementia based on reductions in regional glucose metabolism, cerebral blood flow and cytochrome oxidase activity. *J Neural Transm.* 2004, 111:347-366.

130. Wishkerman A, Greiner S, Ghyczy M, Boros M, Rausch T, Lenhart K and Keppler F: Enhanced formation of methane in plant cell cultures by inhibition of cytochrome c oxidase. *Plant Cell Environ.* 2011*;* 34: 457-464.

131. Wu L and Wang R: Carbon monoxide: endogenous production, physiological functions, and pharmacological applications. *Pharmacol Rev.* 2005; 57:585-630.

132. Yu Y and Pawliszyn J: On-line monitoring of breath by membrane extraction with sorbent interface coupled with CO_2 sensor *J. Chromatogr.* 2004; A 1056:35–41.

133. Zengler K, Richnow HH, Rosselló-Mora R, Michaelis W and Widdel F: Methane formation from long-chain alkanes by anaerobic microorganisms. *Nature*. 1999; 401:266-9.